atmosphere

MDPI

Article

Comprehensive Probabilistic Analysis and Practical Implications of Rainfall Distribution in Pakistan

Fahad Haseeb [1], Shahid Ali [1,*], Naveed Ahmed [2,3], Nassir Alarifi [4] and Youssef M. Youssef [5,*]

[1] Department of Civil Engineering, National University of Computer and Emerging Sciences, Lahore 54770, Pakistan; fahadhaseeb9@gmail.com
[2] The National Key Laboratory of Water Disaster Prevention, College of Hydrology and Water Resources, Hohai University, Nanjing 210098, China; naveedahmed@hhu.edu.cn
[3] College of Hydrology and Water Resources, Hohai University, 1 Xikang Road, Nanjing 210098, China
[4] Department of Geology & Geophysics, College of Science, King Saud University, P.O. Box 2455, Riyadh 11451, Saudi Arabia; nalarifi@ksu.edu.sa
[5] Geological and Geophysical Engineering Department, Faculty of Petroleum and Mining Engineering, Suez University, Suez 43518, Egypt
* Correspondence: shahid.ali@nu.edu.pk (S.A.); youssef.ibrahim@pme.suezuni.edu.eg (Y.M.Y.)

Abstract: Accurately selecting an appropriate probability distribution model is a critical challenge when predicting extreme rainfall in arid and semi-arid regions, especially in countries with diverse climatic conditions. This study presents a comprehensive methodology for evaluating rainfall probability distributions across Pakistan, and aims to create a probabilistic zoning map that could serve as a valuable resource to inform the development of strategies for efficient water resource management and improved flood resilience in diverse climatic and geographic conditions. Precipitation data from the Pakistan Meteorological Department (PMD) over 42 years were compared with CHIRPS, confirming their accuracy. Nine probability distributions were assessed, with five models—log Pearson type-III (LP3), Weibull (W2), log normal (LN2), Generalized Extreme Value (GEV), and gamma (GAM)—deemed most suitable for the region's climatic variability. The spatial applicability of these distributions was identified as follows: LP3 (30%), LN2 (30%), W2 (15%), GEV (10%), and GAM (15%). The central and southern regions of Punjab were predominantly characterized by LN2, while GAM was prevalent in the coastal areas of Sindh. Balochistan exhibited a heterogeneous distribution of W2, LP3, and LN2, while the mountainous Gilgit-Baltistan region was exclusively associated with GEV. Khyber Pakhtunkhwa demonstrated a mix of GEV and LP3 distributions. Beyond provincial variations, distinct patterns emerged: GEV dominated high-altitude, cold-temperate areas; LP3 was common in mountainous regions with variable temperature profiles; and W2 was prevalent along the flood-prone Indus River. This study provides a robust framework for region-specific disaster preparedness and contributes to sustainable development initiatives by offering tailored strategies for managing extreme rainfall events across Pakistan's diverse climatic zones.

Keywords: rainfall analysis; probability distribution; return period; maximum monthly rainfall; annual maxima; extreme events; rainfall distribution

check for updates

Academic Editor: Shanshan Wang

Received: 18 December 2024
Revised: 8 January 2025
Accepted: 21 January 2025
Published: 23 January 2025

Citation: Haseeb, F.; Ali, S.; Ahmed, N.; Alarifi, N.; Youssef, Y.M. Comprehensive Probabilistic Analysis and Practical Implications of Rainfall Distribution in Pakistan. *Atmosphere* **2025**, *16*, 122. https://doi.org/10.3390/atmos16020122

Copyright: © 2025 by the authors. Licensee MDPI, Basel, Switzerland. This article is an open access article distributed under the terms and conditions of the Creative Commons Attribution (CC BY) license (https://creativecommons.org/licenses/by/4.0/).

1. Introduction

Rainfall, a fundamental component of the Earth's hydrological cycle, plays a critical role in influencing climate systems, ecosystems, and human societies. The complex processes governing the formation, distribution, and intensity of rainfall events have been extensively investigated across multiple disciplines, including atmospheric sciences and

hydrology [1]. Understanding the spatial and temporal variability of rainfall patterns, their responses to climate change, and their impact on environmental and socioeconomic systems is essential for addressing key challenges such as water resource management, flood prediction, and agriculture [2].

Globally, sectors dependent on rain-fed systems are structured around natural rainfall patterns [2]. Quantitative measures of precipitation, consisting of average annual rainfall, seasonal distribution patterns, and intensity levels, are critical variables for water resource management, irrigation system design, and for securing urban water supplies [2,3]. However, prolonged intense rainfall elevates flood risks, causing severe infrastructure damage, while insufficient rainfall can lead to droughts and food insecurity in densely populated regions [4]. The variability of rainfall profoundly affects both socioeconomic stability and ecological systems [2]. Extreme precipitation events are a primary driver of flooding, especially in arid and semi-arid developing regions (Figure 1a). Consequently, understanding rainfall distribution trends is essential for strengthening flood-mitigation strategies and optimizing water resource management. Accurate analysis of rainfall distributions hinges on the application of probability distributions to model daily precipitation patterns—a concept extensively investigated in meteorological research to quantify flood risks and forecast extreme weather events [3,5,6].

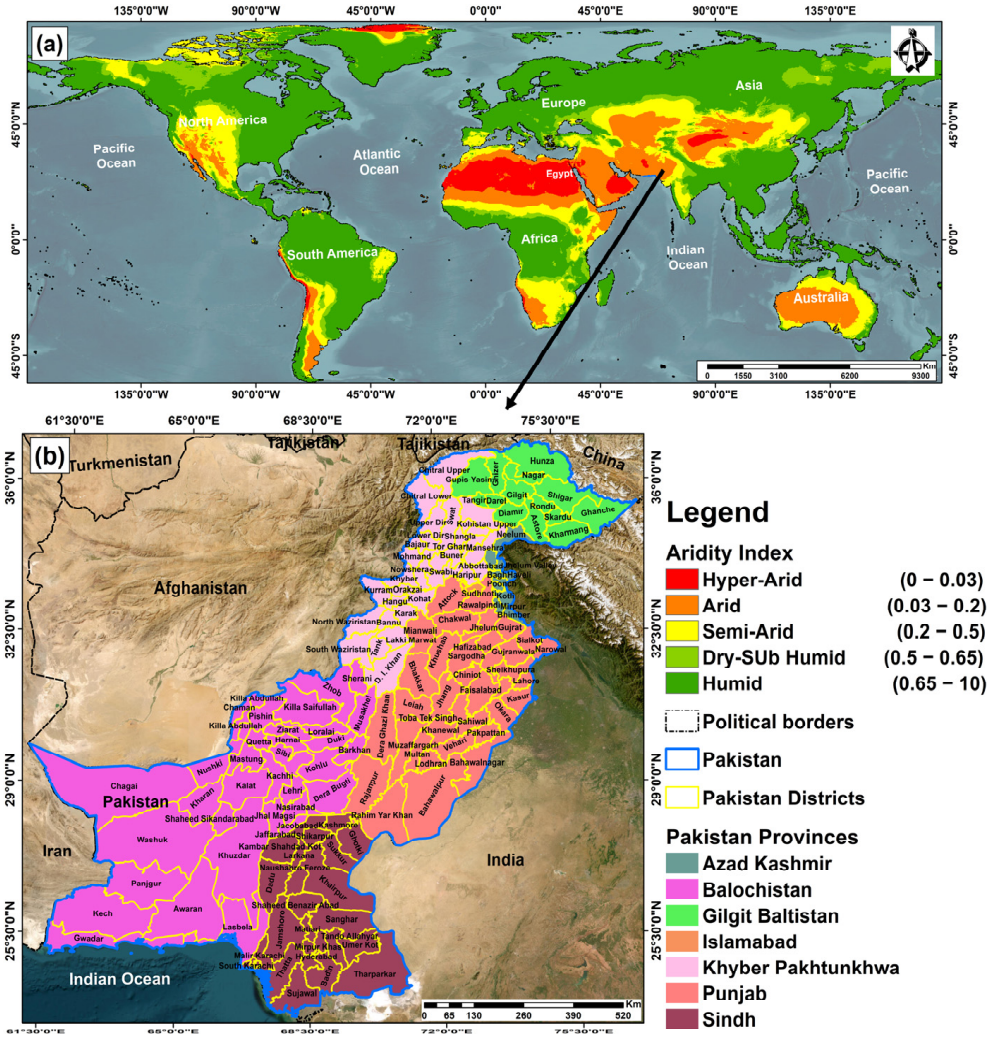

Figure 1. (**a**) Global aridity map illustrating Pakistan's location within the arid to humid zones [7]. (**b**) Map of Pakistan depicting the distribution across provinces and districts, where the analysis in this study is conducted across all districts.

Rainfall replenishes freshwater sources, including lakes and rivers, serving as a critical resource for human, animal, and plant life. However, predicting the occurrence and distribution of rainfall remains a challenge due to its spatiotemporal variability. Analyzing rainfall using probability distributions and annual maximum rainfall data facilitates the efficient management and utilization of water resources [8]. By employing probabilistic and frequency analyses, rainfall extremes corresponding to specific return periods can be estimated [9]. Reliable data on catastrophic events with extended return periods are essential for flood-prevention measures and the design of hydrological infrastructure such as dams, levees, and drainage systems [10].

Various statistical techniques have been developed to forecast rainfall intensity over different durations, accounting for location and time variability [11]. These techniques rely on probability distributions, and numerous studies have been conducted to model rainfall data [12]. Different probability models have been created to depict the distribution of heavy rainfall at a specific location [10,13]. Kumar [14] and Singh [15] demonstrated that the log normal type-2 (LN2) distribution was the best probability distribution for India for the maximum daily annual rainfall. Comparably, Amin et al. [16] deduced that the log Pearson type-3 (LP3) distribution was the best fit for the mountainous northern region of Pakistan. Eslamian et al. [17] deduced that the Generalized Extreme Value (GEV) and the Pearson type-3 (P3) distributions were an accurate demonstration for rainfall in Iran. Likewise, Lee's and Ogunlela's research projects have ascertained that LP3 distributions elegantly summarize the nuanced rainfall dynamics and delineate the peak of daily precipitation [18,19]. Correspondingly, Kwaku and Duke [20] have illuminated LN2 distribution for characterizing the maximum five-day rainfall patterns. A survey conducted has revealed that a substantial 50% of the surveyed weather stations in selected Nigerian cities prefer LP3 distributions, while the remaining 40% opt for Pearson type-3 (P3) distributions to represent the rainfall variations across the region [21]. In the arid landscape of Libya [22], researchers have ascertained that the gamma distribution is the most congruent model for describing monthly peak rainfall. Furthermore, Arora and Singh's meticulous exploration has unveiled the LP3 distribution as the preeminent tool in determining flood frequency, a fact that is duly endorsed by the United States Water Resource Council [23]. Lastly, Moccia's investigation into the distributions characterizing daily rainfall extremes in Italy has illuminated the notable superiority of heavy-tailed distributions over their light-tailed counterparts [24].

The concept of the return period serves as a pivotal tool in delineating the temporal intervals between recurring catastrophic events. The return period elucidates the temporal spacing between the reoccurrences of a given calamity, as characterized by at least the same level of severity and magnitude [25]. This temporal parameter is extracted through the meticulous derivation of quantiles from parametric probability distributions, drawing upon the extreme values encoded within the dataset [26]. The overarching aim of this endeavor is to illuminate the scale and intensity intrinsic to an event recurring within a specified return period. This crucial determination paves the way for the formulation and implementation of targeted mitigation strategies aimed at mitigating the adverse ecological and socioeconomic repercussions wrought by the recurrent event upon the affected region.

Pakistan has experienced severe flooding in the past due to excessive rainfall. In Pakistan, significant disparities exist in the spatial distribution of rainfall. The monsoon season brings over 60% of the annual rainfall to Punjab and Sindh (Figure 1b). Like Balochistan, the northern highlands receive their most rainfall from October to March. Much of the rain in Pakistan is caused by the monsoon winds, western disturbances, and thunderstorms [3]. Unregulated extreme rainfall can cause severe infrastructure damage and economic losses [4,5]. Pakistan's agriculture sector, which significantly contributes to

the national Gross Domestic Product (GDP), is vulnerable to rainfall variability, with many regions relying entirely on precipitation for agricultural activities [16,27]. The intensifying water crisis in Pakistan, driven by climate change, agricultural demands, and inadequate water management strategies, highlights the urgent need for effective mitigation measures and predictive systems [6]. Since 1947, major floods in Pakistan have caused losses exceeding USD 40 billion, with two-thirds of the country being susceptible to flooding [6]. Developing well-defined water management strategies requires an appropriate tool to aid understanding of the spatiotemporal patterns of rainfall distribution in the study region and to enhance the efficacy of flood-mitigation efforts, hence reducing the economic impact of floods on agriculture, infrastructure, and human lives.

Addressing these challenges requires a probabilistic approach to analyzing rainfall patterns and their implications for flood mitigation. To this end, this study aims to develop such an approach by (1) determining the best-fit probability distributions for maximum monthly rainfall across various regions in Pakistan, considering the maximum monthly projected rainfall in the light of critical return periods and (2) introducing probabilistic zoning for the entire country based on comprehensive frequency analysis. Developing a probabilistic zoning map for maximum precipitation across the entire study region will provide a tool that can assist in forming short- and long-term strategies to mitigate the adverse impacts of extreme rainfall events, ensuring more efficient water resource management, and enhanced the resilience to floods. The probabilistic zoning map will be a foundational resource that can identify hotspots prone to extreme events as well as inform development and planning strategies for disaster preparedness and allocation of resources.

2. Data and Methods

2.1. Data and Study Area

Pakistan is on the western side of south Asia and has been spatially divided into five main climatic zones. The topographical features of Pakistan vary from area to area and are extremely diverse in nature (Figure 1b). The northern areas of Pakistan exhibit the three most splendid mountain ranges, i.e., Hindukush, Karakoram, and Himalayas; furthermore, they are the home of a few of the tallest mountains, such as K-2 [28,29]. Not only, this, but the Indus plain was also the home of one of the world's oldest civilizations and has abundantly fertile land. Going towards the south, hot, dry deserts can be found there, and the climate changes with the change in the geography of the country [30].

With the northern areas as an exception where the land witnesses monsoon rainfall of up to 200 mm per month from July to September, the remaining parts of the country receive moderate rainfall [31]. The country faces abundant fluctuations in the annual rainfall because of this, and, hence, is often subjected to extreme droughts and floods happening simultaneously throughout the different regions of the country [31,32]. Furthermore, it has been deduced that during the monsoon season, the flooding reaches its extreme limit and causes an enormous amount of runoff, washing away life and causing large-scale infrastructure damage in critical areas. Table 1 highlights the districts in the region that have recorded rainfall extremes for 24 h (1947–2022), as compiled by the Pakistan Meteorological Department.

Table 1. Extreme rainfall events in Pakistan, compiled by PMD.

Rainfall	District	Province
>400 mm	Islamabad	Punjab
400–300 mm	Rawalpindi Lahore	Punjab
	Jacobabad Naushahro Feroz Tando M. Khan Tharparkar	Sindh
300–200 mm	Dera Ismail Khan Kohat Peshawar Nowshera Abbottabad	Khyber Pakhtunkhwa
	Jhelum Sialkot Sargodha Faisalabad Bahawalnagar	Punjab
	Larkana Shaheed Benazirabad Hyderabad Tando Allahyar Karachi	Sindh
	Gwadar	Balochistan

Given the limitations of ground-based observation data, satellite-derived rainfall estimates have emerged as a valuable alternative or supplementary resource [33–38]. To address the shortcomings of many long-term satellite-based rainfall products, such as coarse spatial and temporal resolutions and non-homogeneity, the Climate Hazards Group InfraRed Precipitation with Station (CHIRPS) dataset, developed by the Climate Hazards Group at the University of California [33], has been employed. CHIRPS is a long-term rainfall dataset that covers over 42 years, from 1981 to 2022, and is available for near global coverage. The ground-based precipitation data for various districts in the region were obtained from the Pakistan Meteorology Department (PMD) and it was compared with the satellite-derived CHIRPS dataset. Both datasets complimented their precipitation values, ensuring the validity and accuracy of the CHIRPS dataset. Utilizing a combination of $0.05^\circ \times 0.05^\circ$ resolution satellite imagery and ground-based station data, CHIRPS generates gridded rainfall time series conducive to trend analysis and seasonal drought monitoring.

Previous research by [39–41] attests to the CHIRPS dataset's comparable performance with widely used satellite products, such as CMORPH, TMPA, PERSIANN, and TRMM, across decadal, monthly, and seasonal time scales in characterizing West African mean precipitation. Additionally, studies conducted by [42,43] have reported satisfactory alignment between the CHIRPS dataset and ground-based observations at 18 daily rain gauge stations in the Sahel and Guinea Coast regions, spanning from 1981 to 2015. This alignment encompasses various aspects, including seasonal precipitation trends, wet-day frequencies, precipitation intensity, and average durations of dry spells.

The accuracy and validity of the CHIRPS dataset have been evaluated and confirmed in various studies. A study utilizing CHIRPS data to validate its accuracy and results demonstrated that CHIRPS performs well in capturing precipitation over different time

scales [44]. However, its accuracy is conditioned by the geographic and climatic characteristics of the region, with somewhat reduced performance in warmer regions. CHIRPS data exhibit strong performance in estimating monthly precipitation, with a correlation coefficient (CC) of 0.89 and minor overestimation of total precipitation [45]. It was, hence, concluded that CHIRPS serves as a reliable alternative source for monitoring drought, with applications across different seasons and regions within Yunnan Province.

These studies collectively highlight CHIRPS as a valuable tool for climate and precipitation analysis, emphasizing its ability to accurately represent precipitation patterns over diverse geographic and climatic regions. CHIRPS stands out as a dependable resource for studying climate variability, seasonal precipitation, and drought occurrences, particularly in areas with limited access to traditional rain gauges.

The graphical representation of the precipitation data for the regions under consideration in the country (30.3753° N, 69.3451° E) is presented in Figure 1. The data obtained represent the precipitation in millimeters and span over the timeline of 42 years from 1981 to 2022. For every month, total rainfall was determined first and then, for each year, the calendar month with the maximum total was selected as having the maximum monthly rainfall (mm/month). By doing so, 42 maxima were generated for every station. For the evaluation of extreme rainfall approximation, this value of maximum monthly rainfall was utilized. The annual maxima (AM) method has been utilized in this study to obtain the extreme rainfall values for further analysis. In this method, the data time-period is divided into regular intervals and the highest value for every interval is selected. In a case when this period is equal to one year, the method is titled the method of annual maxima. Various researchers have used this method in the past to obtain accurate rainfall data for extreme rainfall analysis in their studies [46,47]. These researchers recommend using the annual maxima method rather than the Peak-Over-Threshold (POT) method in the case of rainfall data analysis, as proved by their studies. This method delivers an accurate representation for detailed analysis of extreme precipitation events.

The climatic conditions and geographical features in the climatic zones of Pakistan vary from one another, particularly the rainfall patterns [48]. Various parts of the country experience heavy rainfall that is mainly due to the monsoon and western depression. Therefore, the study area cannot be studied as one single region due to the varying topography and climatic conditions. Considering the spatial division of the region, in the form of climatic zones, was, thus, critical for this study.

The five climatic zones are labelled as A–E, as shown in Figure 2. Zone-A is in the northern part of the country. High-altitude mountains with relatively colder climate throughout the year are the main features of this zone. Similarly, Zone-B is located south of Zone-A, with comparatively sub-mountainous topography along with a moderate cold climate. Zone-C also has a mountainous geography, but it is in the central-western region of the study area. The climate varies in this zone throughout the year, with hot summers and cold winters, developing extreme conditions in both seasons. Zone-D is in the central-eastern region and is mainly known for its dry and extremely hot conditions throughout the year. The conditions are such that the maximum temperature has been recorded several times in the past for the districts located in this zone. Lastly, Zone-E is composed of the southern region of the country. It is the biggest zone in terms of area covered. The coastal area of the zone is located adjacent to the Arabian Sea. However, the condition above the coastal region is mainly arid with a warm and humid climate.

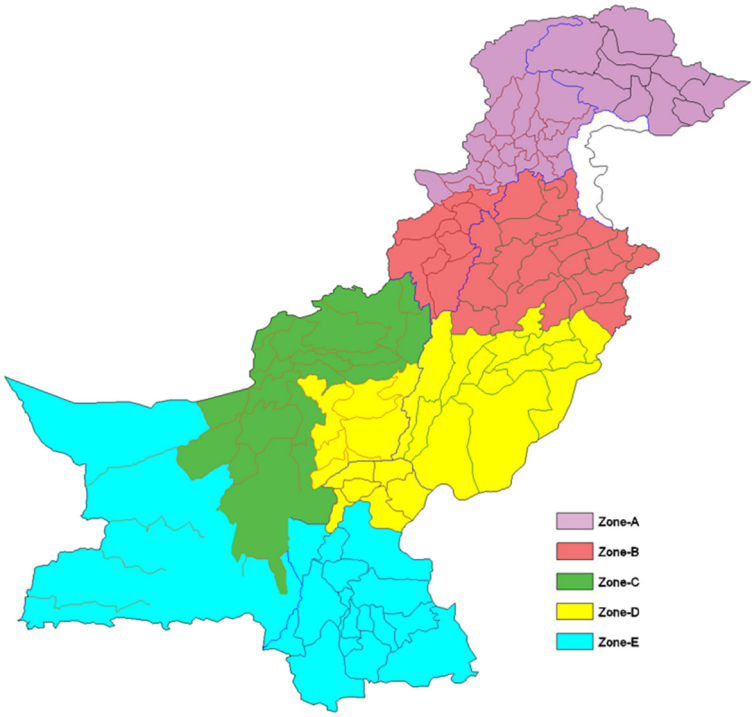

Figure 2. Climate zones of Pakistan.

As per the past records of the different trends of rainfall in the country, it is evident that the maximum rainfall is generated during the monsoon season. As a result of this, if individual districts are analyzed, the maximum monthly rainfall for the past 42 years is witnessed during the months from July to September. In the light of these computations, the best-fit probabilistic distribution zoning map for Pakistan was prepared. Using the results of the comprehensive frequency analysis in the presumptive stage, the concept of probabilistic zoning was implemented. A geographic map of the probability distribution zones was developed. This was the core idea of this research: to develop a probabilistic zoning map using historical rainfall data for Pakistan. Once the map was developed, it was analyzed for correlation with climatic zones and geographic features, and for social impact as well as for policy implications for flood mitigation.

2.2. Methodology

It is evident that the determination of probability distribution model is of immense importance for the accurate representation of the best-fit distribution of selected regions. For this analysis, predefined probability distributions were considered in this study, some of which have been previously used by various researchers for the evaluations of extreme rainfall, but no comprehensive study has been conducted. The estimating strategy, mathematical computations, and procedure for graphical representation of best-fit probability distribution along with the return period have been discussed as follows.

2.2.1. Frequently Used Probability Distributions

As discussed, this approach has been used as a technique to define the frequency distribution for extreme rainfall. To calculate the different distribution parameters, the MOM, commonly known as the methods of moments, was implied. In case of complex situations when MOM estimators are not efficient, L moments are implied, the objective being to determine the parameters for the distribution. L moments are significantly stronger in comparison to the other moments, however, one of the drawbacks of using them for estimation is that they possess extremely low sensitivity.

Using Equations (1)–(3), the sample mean, along with the standard deviation, and, lastly, the coefficient of skewness is determined.

$$\text{Sample mean} = X_{avg} = \frac{\sum X_i}{n} \tag{1}$$

$$\text{Standard deviation} = \sigma = \sqrt{\left[\frac{1}{n-1}\sum\left(X_i - X_{avg}\right)^2\right]} \tag{2}$$

$$\text{Coefficient of skewness} = \gamma = \frac{n.\sum\left(X_i - X_{avg}\right)^3}{(n-1)(n-2)S^3} \tag{3}$$

where N represents the total no. of the readings, I represent the total no. of the observations, and X_i is the observational order of data.

The probability distributions considered in this study are as follows:

(1) Normal distribution: normal distribution (N), also known as the Gaussian distribution, is frequently used in yearly rainfall and runoff studies [49]. Equations (4) and (5) below represent the probability density function along with the cumulative distribution function, respectively.

$$f(x) = \frac{1}{\sigma\sqrt{2\pi}}\exp\left[-\frac{1}{2\sigma^2}(x-\mu)^2\right] \tag{4}$$

$$F(x) = \frac{1}{\sigma\sqrt{2\pi}}\int_{-\infty}^{\infty}\left(\exp\left[-\frac{1}{2\sigma^2}(x-\mu)^2\right]\right)dx \tag{5}$$

keeping in view for the range of $-\infty < x < \infty$.

(2) Log normal distribution: in cases when the range of the random variable "x" exceeds zero. The required distribution functions of the data are stated in Equations (6) and (7), respectively, below.

$$f(x) = \frac{1}{x\sigma_Y\sqrt{2\pi}}\exp\left[-\frac{1}{2\sigma_Y{}^2}(\ln(x)-\mu_Y)^2\right] \tag{6}$$

$$F(x) = \frac{1}{\sigma_Y\sqrt{2\pi}}\int_0^x\left(\frac{1}{x}\exp\left[-\frac{1}{2\sigma_Y{}^2}(\ln(x)-\mu_Y)^2\right]\right)dx \tag{7}$$

the parameter of normal distribution, "x", is represented as y = ln(x) and is computed by considering the MOM. The equations for the two calculated parameters are displayed in Equations (8) and (9) below.

$$\sigma_Y = \sqrt{\ln\left(1+\frac{\sigma_X^2}{\mu_X^2}\right)} \tag{8}$$

$$\mu_Y = \ln(\mu_X) - \frac{1}{2}\sigma_Y^2 \tag{9}$$

the standard deviation is denoted by σ_Y, while the mean is represented by μ_Y.

(3) Pearson type-III distribution: Pearson type-III (P3) is a two-parameter approach and is one of the most popular approaches, especially for the analysis of the hydraulic functions and frequency. Equations (10) and (11) demonstrate the distribution functions.

$$f(x) = \frac{1}{|\alpha|\Gamma(\beta)}\left[\left(\frac{x-\zeta}{\alpha}\right)^{\beta-1}\right]\exp\left[-\left(\frac{x-\zeta}{\alpha}\right)\right] \tag{10}$$

$$F(x) = \frac{1}{|\alpha|\Gamma(\beta)}\int_\zeta^x\left[\left(\frac{x-\zeta}{\alpha}\right)^{\beta-1}\right]\exp\left[-\left(\frac{x-\zeta}{\alpha}\right)\right]dx \tag{11}$$

where shape parameter is denoted by β, scale parameter by α, and position by ζ.

(4) Log Pearson type-III distribution: log Pearson type-III (LP3) distribution demonstrates the logarithm of the different variables of the Pearson type-III distribution. Equations (12) and (13) display the required functions.

$$f(x) = \frac{1}{|\alpha| x \Gamma(\beta)} \left[\left(\frac{\ln(x) - \zeta}{\alpha} \right)^{\beta - 1} \right] \exp\left[- \left(\frac{\ln(x) - \zeta}{\alpha} \right) \right] \tag{12}$$

$$F(x) = \frac{1}{|\alpha| \Gamma(\beta)} \int_0^x \frac{1}{x} \left[\left(\frac{\ln(x) - \zeta}{\alpha} \right)^{\beta - 1} \right] \exp\left[- \left(\frac{\ln(x) - \zeta}{\alpha} \right) \right] dx \tag{13}$$

(5) Exponential distribution: exponential distribution (EXP) is another distribution technique belonging to the gamma family. The probability density function as well as the cumulative distribution function are, respectively, demonstrated in Equations (14) and (15) below.

$$f(x) = \alpha^{-1} \exp\left[- \left(\frac{x - \zeta}{\alpha} \right) \right] \tag{14}$$

$$F(x) = 1 - \exp\left[- \left(\frac{x - \zeta}{\alpha} \right) \right] \tag{15}$$

similar to the MOM estimators in the above distribution techniques, the L-moment estimators in the exponential distribution predict the position, ζ, and shape parameters, α, where λ_1 is the mean of the dataset and λ_2 is the exponential distribution's L-scale.

(6) Gumbel distribution: Gumbel distribution (GUM) is the type-I of extreme value distribution used to evaluate the maximum value in terms of the dataset, for example, the maximum discharge. The probability density function and the cumulative distribution function are exhibited in Equations (16) and (17) below.

Furthermore, the distribution scale parameter α and the location parameter β are calculated by the MOM estimators for the GUM distribution.

$$f(x) = \left(\frac{1}{\alpha} \right) \exp\left[- \left(\frac{x - \beta}{\alpha} \right) - \exp\left(- \left(\frac{x - \beta}{\alpha} \right) \right) \right] \tag{16}$$

$$F(x) = \exp\left[- \exp\left(- \frac{x - \beta}{\alpha} \right) \right] \tag{17}$$

(7) Generalized Extreme Value distribution: unlike Gumbel distribution, the Generalized Extreme Value distribution (GEV) is a three-parameter distribution. This distribution is suggested by several European Nations to provide the most accurate evaluation of the flood statistics [50].

For the evaluation of the parameters, the L estimators are used instead of the MOM. It has a geometry, κ, a scale, α parameter, and position, ζ. Equations (18)–(21) represent the probability density function and the cumulative distribution function, respectively.

$$f(x) = \alpha^{-1} \exp[-(1 - k)y - exp(-y)] \tag{18}$$

$$y = -k^{-1} \log\left[1 - \frac{k(x - \zeta)}{\alpha} \right], \; k \neq 0 \tag{19}$$

$$y = \frac{x - \zeta}{\alpha}, \; k = 0 \tag{20}$$

$$F(x) = \exp[-exp - y] \tag{21}$$

(8) Weibull distribution: the Weibull probability distribution is a cornerstone of the domain of hydrology, playing a pivotal role in the analysis of rainfall frequencies and flood

magnitudes. According to the research conducted by Stendinger et al. [51], it has been deduced that the Weibull (W2) frequency distribution is regularly used for the frequency distribution characteristics in hydraulics. Equations (22) and (23) represent the probability density function and the cumulative distribution function, respectively. For the calculation of the parameters with this distribution, the MOM estimators are used.

$$f(x) = \left(\frac{k}{\alpha}\right)\left(\frac{x}{\alpha}\right)^{k-1} \exp\left[-\left(\frac{x}{\alpha}\right)^{k}\right] \quad (22)$$

$$F(x) = 1 - \exp\left[-\left(\frac{x}{\alpha}\right)^{k}\right] \quad (23)$$

(9) Gamma distribution: the gamma probability distribution holds paramount importance in the realm of hydrology, particularly in the analysis of rainfall frequency and flood occurrences. The profound influence of gamma distribution resonates throughout hydrological research, underpinning crucial decisions in flood management, urban planning, and disaster preparedness [52].

The gamma probability density function and cumulative distribution function are described by Equations (24) and (25), respectively, wherein γ denotes the shape parameter, β signifies the scale parameter, x represents a specific rainfall amount, and μ is the location parameter. The evaluation or estimation of the complete gamma function (Γ) can be accomplished using tables readily available in various software packages or through mathematical equation, as mentioned in Equation (26).

$$f(x) = \frac{\left(\frac{x-\mu}{\beta}\right)^{\gamma-1} e^{\left(-\frac{x-\mu}{\beta}\right)}}{\beta\Gamma(\gamma)} \; x \geq \mu; \gamma, \beta > 0 \quad (24)$$

$$F(x) = \frac{\Gamma_x(\gamma)}{\Gamma(\gamma)} \; x \geq 0; \; \gamma > 0 \quad (25)$$

$$\Gamma(a) = \int_0^\infty t^{a-1} e^{-t} dt \quad (26)$$

2.2.2. Goodness-of-Fit Test

Utilizing goodness-of-fit tests, the selected distribution system model undergoes validation, a crucial step in our analysis. This validation encompasses three distinct techniques for assessing normality from various vantage points. First, we employ graphical approaches, including histograms, Q-Q Plots, and box plots. Subsequently, we delve into numerical methods, encompassing the scrutiny of skewness and kurtosis indices and the application of formal normality tests. These tests incorporate the empirical distribution function (EDF) tests, facilitating a rigorous comparison between actual and theoretical distributions [53]. The few of the renowned EDF tests include the Kolmogorov–Smirnov, also known as the K–S, Anderson–Darling, commonly known as the A–D, Cramer Von Mises, and root mean square error [54,55]. In this research, the Kolmogorov–Smirnov (K–S), Anderson–Darling (A–D), and root mean square error tests have been used to assist us to determine the best-fit probability distribution for the region. For the graphical representation of results, the Q-Q plots were prepared.

(1) Kolmogorov–Smirnov (K–S) test: it is the type of EDF test where the maximum vertical deflection in the theoretical versus the actual distribution is demonstrated [56]. The core objective of using the EDF approach is to evaluate the empirical cumulative frequency ($S_n(x)$) of the cumulative density function of a hypothetical distribution ($F_x(x)$). The K–S test statistic is the maximum vertical gap between $S_n(x)$ and $F_X(x)$. The data are organized in ascending order, where n is the total number of the samples in the dataset. Using this

information, the K–S value is calculated for each sorted value of n. Equations (27a–c)–(29) represent the calculation for the value of S_n, D_n, and corresponding probability.

$$S_n(x) = 0; \text{if } X < X_1 \tag{27a}$$

$$S_n(x) = \frac{k}{n}; \text{if } X_k \leq X < X_{k+1} \tag{27b}$$

$$S_n(x) = 1; \text{if } X > X_n \tag{27c}$$

$$D_n = \max|F_x(x) - S_n(x)| \tag{28}$$

$$P(D_n \leq D_n^{\alpha}) = 1 - \alpha \tag{29}$$

where D_n^{α} is the critical value.

(2) Anderson–Darling (A–D) test: the A–D. Anderson–Darling test was developed by Anderson and Darling [57] and is the most effective EDF test to give additional weight to the tails of the distribution [58]. This type of EDF test is the most effective testing method for data with big extremes, hence, it is efficient when developing the best-fitting model. The quadratic category of EDF is represented by A^2 in this test method and is calculated through the equation demonstrated in (30).

$$A^2 = -\frac{\sum[(2i-1)\ln F_X(x_i) + \ln[1 - F_X(x_{n+1-i})]]}{n} - n \tag{30}$$

One of the points to ponder in this test is that it should be ensured that the n are arranged in ascending order. Unlike the Kolmogorov–Smirnov (K–S) test, the A–D test, on the other hand, assigns more weight to the tails, hence, it is more appropriate for the dataset with extreme values. Therefore, this method is more appropriate with respect to the accurate demonstration of the results.

(3) Root mean square error (RMSE): the root means square error, also known as the RMSE, is the value that exhibits the best-fit model of the variation and denotes the standard deviation of the predicted error. As a result of this, the difference between the calculated and the predicted value is found out. Equation (31) displays the formula used to calculate the root mean square error (RMSE).

$$RMSE = \sqrt{\frac{1}{n}\Sigma(x_i - X)^2} \tag{31}$$

From the above equation, the estimated value is denoted by x_i, while, on the other hand, the recorded data value is represented by X.

(4) Graphical test: as discussed, one of the methods for the goodness-of-fit tests is the graphical approach. This test is the most up to a point and straightforward, yet it is one of the most effective methods to determine the best-fit model. The graphical method used for this research is the Q-Q plotting approach of the measured as well as the predicted value. With the help of various plotting positions formulae, the non-exceedance probability, denoted by $P_{i:n}$, is calculated. The equation to calculate the $P_{i:n}$ is demonstrated in Equation (32) below.

$$p_{i:n} = \frac{n - a}{N + 1 - 2a} \tag{32}$$

Looking at the above equation, the rank of the recorded values, X, is expressed by n, while the total number of the recorded values in denoted by N. Throughout the formula, the constant value is denoted by "a".

2.2.3. Return Period

The determination of the return period stands as a pivotal component in the examination of any exceptional flood event. This calculation serves a dual purpose: firstly, it enables the estimation of the anticipated magnitude of the impending catastrophic occurrence. Secondly, it provides the relevant authorities with a temporal window for the implementation of imperative measures aimed at mitigating the adverse consequences of the impending disaster.

Equation (34) exhibits the calculation of the return period, where x_T is the magnitude of the event, while the probability of the occurrence of the event is denoted by P(X > x) for each year in Equation (33).

$$P(x \geq x_T) = \frac{1}{T} \tag{33}$$

$$T = \frac{1}{1 - P(x \leq x_T)} \tag{34}$$

It should be noted that the rainfall levels for both 50- and 100-year recurrence internals cannot be represented accurately from the dataset, however, the data can be retrieved from the 98th and 99th percentiles, respectively, of the best-fitted distribution [26].

3. Results and Discussion

The main objective of the research was to determine the best-fit probability distribution for the specified regions that record the highest monthly rainfall data in order to predict the recurrence of the flooding event for time intervals ranging from 10, 25, 50, to 100 years, respectively.

With the help of the results, the concerned governing bodies and policymakers will be given the projected insights for the event to help them make better decisions and take efficient steps to cater with the disastrous events. The goal of this research is to help policymakers to take steps to minimize the impact of such circumstances, and to enable the degree of risk to be evaluated for extreme events like rainfall and corresponding flooding.

3.1. Selection the Best-Fit Distribution Results

The probabilistic analysis revealed that the rainfall distribution ranges widely across all districts in the region. The geographical specifics of the site, such as longitude, latitude, and elevation, as well as the surrounding climatic conditions, all contribute to rainfall variance. The northeastern part of Pakistan receives the most measured precipitation; for example, the Islamabad district has recorded a maximum monthly rainfall of 1023 mm over the past 42 years. The districts in Pakistan's southeastern area reported the least amount of precipitation when compared to the other locations (such as Larkana district, with an 80.9 mm monthly maximum). The district names, statistical summary findings, best-fit K–S, A–D, RMSE, and best-scored outcomes are all detailed in Table 2. The probability distribution with the lowest goodness-of-fit among all probability distributions constructed for each district is defined as the best-fit outcome for that district. For each model selection tool, the table presents the best-fit distribution-type test statistic result in terms of probability (K–S, A–D, RMSE). Each selection tool scores all probability distributions that have been constructed (rank 1 is the best fit). A ranking score for the highest ranked distribution is calculated by adding the three ranking results of the goodness-of-fit tests together. As the best-fit distribution model, the distribution model with the lowest ranking score for each district is selected.

Table 2. (**a**) Statistical results and best-fit results for the districts of Punjab. (**b**) Statistical results and best-fit results for the districts of Sindh. (**c**) Statistical results and best-fit results for the districts of Balochistan. (**d**) Statistical results and best-fit results for the districts of Khyber Pakhtunkhwa. (**e**) Statistical results and best-fit results for the districts of Gilgit-Baltistan.

(**a**)

Dt. No	District Name	Mean	SD	Coeff. of Skew.	Best-Fit Test Statistic Results			Highest Ranked Distribution (Sum of Ranks)
					By K–S Test	By A–D Test	By RMSE Test	
1	Attock	168.9	45.9	0.608	W2(0.047)	LP3(0.35)	LP3(7.13)	LP3(4)
2	Bahawalnagar	66.2	30.9	1.728	W2(0.117)	W2(0.20)	LN2(9.60)	LN2(6)
3	Bahawalpur	72.0	37.8	1.839	W2(0.138)	EXP(0.19)	LN2(11.65)	LN2(5)
4	Bhakkar	93.1	39.1	0.970	W2(0.084)	GEV(0.18)	LN2(5.27)	LN2(6)
5	Chakwal	188.5	45.6	0.363	W2(0.041)	LP3(0.47)	LN2(7.97)	LN2(7)
6	DeraGhaziKhan	74.3	34.7	1.086	W2(0.099)	GAM(0.15)	LN2(4.85)	LN2(6)
7	Faisalabad	180.4	51.7	0.123	GAM(0.033)	LP3(0.28)	LP3(5.65)	GAM(6)
8	Gujranwala	183.2	52.7	0.631	W2(0.055)	LP3(0.29)	LN2(7.82)	LN2(6)
9	Gujrat	292.8	72.9	0.248	W2(0.042)	LP3(0.44)	LP3(8.12)	LP3(4)
10	Hafizabad	170.0	49.4	0.567	GUM(0.003)	LP3(0.28)	LN2(6.85)	LN2(7)
11	Jhang	76.8	30.1	0.900	W2(0.074)	GEV(0.06)	LN2(4.10)	LN2(6)
12	Jhelum	292.7	85.0	0.356	GAM(0.025)	LP3(0.27)	LP3(15.80)	LP3(4)
13	Kasur	141.2	48.2	0.493	GAM(0.029)	LP3(0.06)	LP3(9.30)	GAM(6)
14	Khanewal	52.3	24.6	1.309	W2(0.102)	W2(0.08)	LN2(3.61)	LN2(6)
15	Khushab	136.4	41.6	0.757	W2(0.060)	LP3(0.22)	LN2(6.47)	LN2(5)
16	Lahore	429.5	127.0	0.534	W2(0.058)	LP3(0.25)	LN2(15.21)	LN2(7)
17	Layyah	75.4	33.3	1.280	W2(0.096)	EXP(0.06)	LN2(5.44)	LN2(6)
18	Lodhran	48.7	26.7	1.725	W2(0.136)	EXP(0.30)	LN2(7.43)	LN2(7)
19	Mandi Bahauddin	181.2	44.2	1.024	W2(0.047)	LP3(0.49)	LP3(10.18)	LP3(4)
20	Mianwali	152.1	51.6	1.140	W2(0.077)	LP3(0.12)	LP3(10.33)	LP3(4)
21	Multan	81.7	39.9	2.007	W2(0.124)	LN2(0.25)	W2(9.48)	LN2(6)
22	Muzaffargarh	50.4	25.0	1.259	W2(0.103)	W2(0.11)	LN2(4.38)	LN2(6)
23	NankanaSahib	139.3	51.8	0.679	W2(0.071)	LP3(0.06)	LN2(7.07)	LN2(5)
24	Narowal	308.1	107.0	−0.059	GAM(0.047)	LN2(0.13)	LP3(16.72)	GAM(6)
25	Okara	90.4	33.7	−0.230	GAM(0.055)	EXP(0.05)	GUM(4.14)	GAM(7)
26	PakPattan	73.4	30.6	0.807	GAM(0.024)	EXP(0.07)	LP3(6.93)	GAM(7)
27	RahimYarKhan	51.1	32.4	2.109	W2(0.180)	EXP(0.45)	LN2(7.87)	LN2(6)
28	Rajanpur	54.1	32.8	2.336	W2(0.172)	EXP(0.29)	W2(9.19)	W2(4)
29	Rawalpindi	313.6	80.2	0.307	GAM(0.023)	LP3(0.41)	LP3(12.27)	LP3(4)
30	Sahiwal	71.7	30.7	0.689	GAM(0.034)	EXP(0.14)	LP3(5.22)	GAM(6)
31	Sargodha	132.6	36.6	0.476	GAM(0.024)	LP3(0.33)	LN2(4.35)	GAM(7)
32	Sheikhupura	181.2	55.8	0.270	GAM(0.030)	LP3(0.19)	LP3(7.15)	GAM(5)
33	Sialkot	293.5	80.8	0.234	W2(0.052)	LP3(0.33)	LP3(11.10)	LP3(4)
34	TobaTekSingh	65.9	24.9	0.812	GAM(0.021)	LP3(0.08)	LN2(3.71)	GAM(7)
35	Vehari	51.5	26.0	1.884	GAM(0.019)	EXP(0.11)	LN2(6.70)	GAM(5)
36	Islamabad	329.5	93.7	0.400	GAM(0.024)	LP3(0.29)	LP3(17.46)	LP3(4)

Table 2. *Cont.*

(**b**)

Dt. No	District Name	Mean	SD	Coeff. of Skew.	Best-Fit Test Statistic Results			Highest Ranked Distribution (Sum of Ranks)
					By K–S Test	By A–D Test	By RMSE Test	
1	Badin	101.3	66.6	0.696	GAM(0.041)	W2(0.43)	LP3(8.70)	GAM(7)
2	Dadu	51.1	46.5	2.752	GAM(0.100)	LP3(2.14)	LN2(14.38)	LP3(6)
3	Ghotki	45.8	34.5	1.689	LN2(0.014)	GUM(1.88)	LN2(5.23)	LN2(4)
4	Hyderabad	82.0	60.5	0.826	GAM(0.077)	GUM(1.74)	LP3(9.67)	GAM(6)
5	Jacobabad	32.3	25.0	3.179	GAM(0.095)	GAM(1.94)	LP3(9.55)	LP3(6)
6	Jamshoro	76.1	60.6	1.404	GAM(0.031)	GAM(1.55)	LP3(11.85)	GAM(4)
7	Karachi	89.9	70.4	1.473	GAM(0.035)	GAM(1.48)	LN2(12.56)	GAM(4)
8	Kashmore	31.9	21.6	2.540	GUM(0.031)	GUM(1.54)	W2(6.09)	W2(6)
9	Khairpur	76.9	59.5	1.376	GUM(0.015)	GUM(2.09)	LN2(7.50)	LN2(7)
10	Larkana	28.3	22.7	2.952	GUM(0.039)	LP3(1.12)	LP3(7.73)	LP3(4)
11	Matiari	75.7	58.0	1.099	GUM(0.057)	LN2(2.44)	LP3(8.09)	LP3(6)
12	Mirpurkhas	102.0	68.8	0.844	LN2(0.064)	LN2(1.95)	LP3(9.84)	LN2(4)
13	Naushahro Feroze	54.6	52.3	2.872	GUM(0.026)	LP3(1.76)	LN2(14.2)	LP3(7)
14	Qambar Shahdadkot	28.4	20.0	3.070	LN2(0.043)	LN2(0.81)	LP3(7.29)	LP3(6)
15	Sanghar	96.2	70.6	1.144	GUM(0.024)	LN2(1.85)	LP3(11.24)	LN2(7)
16	Shaheed Benazirabad	70.0	57.8	1.527	LN2(0.040)	W2(2.03)	LP3(9.79)	W2(7)
17	Shikarpur	27.3	19.8	2.560	LN2(0.034)	GUM(1.63)	W2(6.16)	LN2(6)
18	Sukkur	48.2	38.6	1.930	GAM(0.043)	GUM(1.85)	LN2(7.10)	LN2(7)
19	Tando Allahyar	89.6	63.7	0.844	LN2(0.077)	GUM(1.95)	LP3(9.69)	LN2(7)
20	Tando M. Khan	86.4	60.4	0.867	LN2(0.087)	GAM(1.08)	LP3(8.78)	GAM(6)
21	Tharparkar	136.5	77.3	0.539	GAM(0.046)	GUM(1.06)	LP3(11.37)	GAM(7)
22	Thatta	103.2	76.4	1.286	LN2(0.083)	GAM(1.27)	LP3(14.79)	GAM(5)
23	Umerkot	103.2	69.1	1.043	GAM(0.031)	W2(0.61)	LP3(10.62)	GAM(7)

(**c**)

Dt. No	District Name	Mean	SD	Coeff. of Skew.	Best-Fit Test Statistic Results			Highest Ranked Distribution (Sum of Ranks)
					By K–S Test	By A–D Test	By RMSE Test	
1	Awaran	46.5	40.4	3.510	W2(0.311)	EXP(0.69)	LP3(14.36)	W2(5)
2	Barkhan	108.5	54.4	1.123	W2(0.118)	W2(0.06)	LN2(6.17)	LN2(6)
3	Chagai	26.9	13.5	1.712	LP3(0.019)	EXP(0.150)	LP3(3.05)	LP3(4)
4	Chaman	69.5	26.7	0.806	LP3(0.016)	N(0.09)	LN2(3.08)	LP3(6)
5	Dera Bugti	50.4	35.0	1.820	W2(0.180)	EXP(0.76)	LP3(7.03)	W2(7)
6	Dukki	61.6	26.6	1.178	N(0.024)	GEV(0.23)	LN2(4.59)	LN2(7)
7	Gawadar	30.3	14.0	1.589	N(0.036)	EXP(0.06)	LP3(2.47)	LP3(5)
8	Harnai	73.3	31.7	1.343	W2(0.090)	LN2(0.19)	LP3(5.31)	W2(6)
9	Jafarabad	31.9	23.8	3.354	W2(0.231)	EXP(0.39)	LP3(9.44)	W2(7)
10	Jhal Magsi	34.5	27.1	3.410	W2(0.263)	EXP(0.48)	LP3(10.33)	W2(6)
11	Kachhi	38.9	21.9	2.525	W2(0.131)	W2(0.8)	W2(6.38)	W2(3)

Table 2. *Cont.*

(**c**)

Dt. No	District Name	Mean	SD	Coeff. of Skew.	Best-Fit Test Statistic Results			Highest Ranked Distribution (Sum of Ranks)
					By K–S Test	By A–D Test	By RMSE Test	
12	Kalat	41.8	20.6	1.330	N(0.035)	W2(0.10)	LP3(3.73)	LP3(5)
13	Kech	34.3	17.5	1.965	LP3(0.017)	LP3(0.42)	W2(4.46)	LP3(4)
14	Kharan	32.7	14.6	1.059	LP3(0.024)	LP3(0.34)	LN2(2.75)	LP3(4)
15	Khuzdar	49.5	32.9	3.073	W2(0.141)	EXP(0.23)	LP3(11.42)	W2(5)
16	Kohlu	81.6	43.4	1.531	W2(0.134)	W2(0.29)	LN2(8.52)	W2(4)
17	Lasbela	59.1	50.0	2.313	W2(0.265)	EXP(1.04)	W2(14.83)	W2(4)
18	Loralai	69.7	29.9	0.812	LN2(0.015)	EXP(0.12)	LN2(5.13)	LN2(4)
19	Mastung	56.2	24.9	1.271	LP3(0.016)	LP3(0.29)	LP3(3.85)	LP3(3)
20	Musakhel	105.7	42.3	0.773	N(0.024)	GEV(0.13)	LN2(5.12)	LN2(6)
21	Nasirabad	30.1	22.7	3.322	W2(0.133)	EXP(0.41)	LP3(9.01)	W2(5)
22	Nushki	45.3	19.7	0.891	LP3(0.019)	EXP(0.12)	LN2(2.78)	LP3(5)
23	Panjgur	33.6	24.4	2.580	W2(0.210)	LP3(1.02)	W2(6.73)	LP3(7)
24	Pishin	80.2	35.0	1.865	LP3(0.014)	W2(0.08)	LP3(8.77)	LP3(4)
25	Qilla Abdullah	72.0	31.2	1.156	LP3(0.016)	LP3(0.27)	LP3(5.68)	LP3(3)
26	Qilla Safiullah	51.3	17.9	1.468	LP3(0.010)	LP3(0.12)	LP3(3.32)	LP3(3)
27	Quetta	68.6	30.1	1.440	LP3(0.018)	LP3(0.25)	LP3(5.77)	LP3(3)
28	Sherani	78.8	25.7	0.505	LP3(0.010)	LN2(0.08)	LN2(3.52)	LN2(4)
29	Sibi	50.1	26.2	1.838	W2(0.123)	W2(0.40)	LP3(5.52)	W2(4)
30	Sohbatpur	35.0	24.9	2.485	W2(0.190)	W2(1.49)	W2(7.34)	W2(3)
31	Surab	38.0	20.1	1.506	LP3(0.015)	W2(0.28)	LN2(3.59)	LP3(6)
32	Washuk	26.6	12.1	1.165	LP3(0.020)	GAM(0.12)	LN2(1.78)	LP3(7)
33	Zhob	56.8	17.0	0.710	GAM(0.020)	GUM(0.21)	LN2(2.11)	LN2(7)
34	Ziarat	68.4	25.0	1.156	W2(0.069)	GUM(0.09)	LP3(4.59)	LP3(6)

(**d**)

Dt. No	District Name	Mean	SD	Coeff. of Skew.	Best-Fit Test Statistic Results			Highest Ranked Distribution (Sum of Ranks)
					By K–S Test	By A–D Test	By RMSE Test	
1	Abbottabad	335.3	91.6	0.997	W2(0.06)	GUM(0.32)	LN2(21.1)	LN2(6)
2	Bajaur	155.0	45.2	0.191	W2(0.046)	LP3(0.26)	LP3(5.54)	LP3(4)
3	Bannu	102.9	28.6	1.403	W2(0.049)	LP3(0.38)	LP3(7.38)	LP3(4)
4	Battagram	208.5	46.9	0.931	W2(0.041)	GEV(0.61)	LP3(8.65)	GEV(5)
5	Buner	245.6	72.1	1.357	W2(0.07)	LP3(0.32)	LP3(16.21)	LP3(4)
6	Charsadda	124.7	34.6	0.834	W2(0.053)	LP3(0.34)	LN2(8.03)	LP3(5)
7	Chitral	84.5	24.1	0.506	W2(0.044)	GEV(0.37)	LN2(3.84)	GEV(6)
8	Dera Ismail Khan	89.5	38.9	1.536	W2(0.102)	GAM(0.07)	LP3(8.59)	GAM(5)
9	Dir	172.7	47.7	0.405	W2(0.046)	GEV(0.41)	N(6.85)	GEV(5)
10	Hangu	134.7	40.5	0.947	LP3(0.017)	LP3(0.26)	LP3(7.22)	LP3(3)

Table 2. *Cont.*

(**d**)

Dt. No	District Name	Mean	SD	Coeff. of Skew.	Best-Fit Test Statistic Results			Highest Ranked Distribution (Sum of Ranks)
					By K–S Test	By A–D Test	By RMSE Test	
11	Haripur	251.3	69.7	0.653	W2(0.053)	LP3(0.33)	LN2(13.38)	LN2(5)
12	Karak	149.3	48.8	1.036	LN2(0.018)	LP3(0.16)	LP3(7.59)	LP3(4)
13	Khyber	130.5	35.9	0.484	LP3(0.009)	LP3(0.33)	LN2(3.95)	LP3(4)
14	Kohat	139.1	39.6	0.735	W2(0.049)	LP3(0.31)	LP3(6.72)	LP3(4)
15	Kohistan	108.6	24.0	0.738	LN2(0.008)	GEV(0.62)	LP3(4.28)	GEV(5)
16	Kurram	126.0	34.3	0.339	LP3(0.013)	LP3(0.17)	LP3(6.15)	LP3(3)
17	Lakki Marwat	114.0	37.9	1.344	LP3(0.013)	LP3(0.17)	LP3(7.58)	LP3(3)
18	Malakand	187.8	55.7	0.793	LP3(0.012)	GEV(0.33)	LN2(9.32)	GEV(5)
19	Mansehra	202.9	43.1	1.040	LP3(0.007)	GEV(0.65)	LP3(9.29)	GEV(6)
20	Mardan	180.4	55.1	0.918	W2(0.062)	GEV(0.30)	LP3(9.02)	GEV(6)
21	Mohmand	125.2	41.9	0.640	LP3(0.011)	GEV(0.18)	LN2(4.29)	LN2(5)
22	North Waziristan	94.9	23.5	0.926	W2(0.036)	LP3(0.47)	LP3(3.77)	LP3(4)
23	Nowshera	137.9	38.5	0.854	LP3(0.010)	LP3(0.34)	LP3(5.78)	LP3(3)
24	Orakzai	138.1	35.6	0.340	LP3(0.014)	LP3(0.40)	LP3(5.03)	LP3(3)
25	Peshawar	108.6	31.0	0.883	LP3(0.010)	LP3(0.32)	LN2(6.97)	LP3(4)
26	Shangla	179.4	42.6	1.302	W2(0.043)	GEV(0.56)	LP3(8.75)	GEV(7)
27	South Waziristan	80.4	23.1	1.035	LP3(0.01)	GEV(0.37)	LP3(4.60)	LP3(4)
28	Swabi	216.1	63.1	0.901	LP3(0.008)	GEV(0.35)	LN2(10.19)	LP3(7)
29	Swat	125.7	31.0	0.889	LP3(0.011)	GEV(0.56)	LP3(4.19)	GEV(6)
30	Tank	90.8	36.6	1.113	W2(0.083)	GAM(0.11)	LN2(5.63)	GAM(7)

(**e**)

Dt. No	District Name	Mean	SD	Coeff. of Skew.	Best-Fit Test Statistic Results			Highest Ranked Distribution (Sum of Ranks)
					By K–S Test	By A–D Test	By RMSE Test	
1	Astore	101.2	29.3	1.0	GEV(0.008)	LP3(0.25)	GEV(5.47)	GEV(4)
2	Diamer	120.5	37.6	0.7	GEV(0.009)	LN2(0.19)	GEV(5.61)	GEV(4)
3	Ghanche	54.8	20.6	0.4	LP3(0.008)	GEV(0.10)	LN2(3.28)	GEV(7)
4	Ghizer	59.8	19.2	0.9	GUM(0.006)	GEV(0.39)	LN2(2.86)	GEV(7)
5	Gilgit	52.2	15.0	1.6	LP3(0.011)	GEV(0.26)	GEV(3.73)	GEV(4)
6	Hunza	43.5	12.1	1.9	GEV(0.018)	GEV(0.49)	LP3(2.44)	GEV(4)
7	Kharmang	94.4	34.1	1.0	GEV(0.012)	LN2(0.07)	GEV(6.12)	GEV(4)
8	Nagar	42.8	13.8	0.6	LP3(0.005)	GEV(0.11)	GEV(1.96)	GEV(4)
9	Shigar	53.9	15.4	0.6	GEV(0.004)	GEV(0.27)	GEV(2.05)	GEV(3)
10	Skardu	78.9	24.8	0.9	GEV(0.009)	GEV(0.08)	GEV(4.45)	GEV(3)

The outcomes presented in Table 2 encompass the statistical parameters pertaining to all districts, encompassing measures of central tendency, dispersion, and the degree of asymmetry. Notably, the skewness coefficient within this analysis yields negative values exclusively for two districts, Okara and Narowal, while the remainder exhibit a positive skewness coefficient. Positive skewness is characteristic of distributions with pronounced right-tailedness, indicating heightened instances of intense rainfall in this

context. The magnitude of skewness serves as a quantification of the extent to which data points deviate from the central average. Approximately 52% of the nation's districts, specifically 69 out of 133, manifest skewness coefficients surpassing one, underscoring a pronounced asymmetry relative to the mean. In contrast, 46 districts display moderately skewed values ranging between 0.5 and 1. Furthermore, a subset of eighteen districts demonstrates near-symmetrical distributions with skewness values spanning from −0.5 to 0.5.

Table 2 presents comprehensive statistical outcomes from the goodness-of-fit tests, including the Kolmogorov–Smirnov (K–S), Anderson–Darling (A–D), and root mean square error (RMSE) tests. Notably, LP3 emerged as the most suitable distribution across the entire study area, encompassing 46 districts, with LN2 ranking as the second most prevalent choice, adopted by 33 districts (as depicted in Table 2). Remarkably, these two distributions collectively accounted for nearly 60% of the regions under investigation. The remaining 40% of the districts exhibited preferences for GAM, GEV, and W2, with 20, 19, and 15 districts, respectively, aligning with each. In total, nine different distributions were considered for rainfall data analysis, with five of them emerging as the optimal fits for various districts within the region. Conversely, the remaining four distributions, namely EXP, N, P3, and GUM, were integrated into the analysis but did not secure recognition as the most appropriate probability distributions during the scrutiny process.

A variation in the results was observed in the three goodness-of-fit tests with respect to the different situations. To summarize this, a ranking system was developed to short list the best-fit distribution for each of the different stations. Moreover, keeping everything in view, the numerical test is just as important as the graphical observation in determining the best-fit probability model. The RMSE was used to determine the distribution fit with the observed data for all districts' Q-Q plots. As an example, Figure 3 depicts the plots for the Lahore district.

The primary aim of fitting probability distributions is to provide a precise portrayal of the probability distribution with low scores on the far-right tail. To assess the quality of fit in this tail region, the Q-Q plot offers a valuable tool [59,60]. In this plot, exact matches between observed data points align precisely with the [1:1] reference line. As depicted in Figure 3, the LN2 distribution demonstrates a well-fitted representation, with the right tail closely aligned with the [1:1] line. However, across the other districts, no consistent pattern emerged for any specific distribution. In these cases, the right tail often exhibited underestimations or overestimations. Across all districts, the W2, LP3, LN2, GAM, or GEV distributions displayed superior performance in capturing the best-fit probability distribution for their respective districts.

The information conveyed in Table 1 illustrates the most suitable probability distribution for each district within the region. Nevertheless, the full scope of this investigation necessitates a graphical representation of these outcomes. This study aimed to construct a probabilistic zoning map utilizing the historical rainfall data and this concept was translated into practical implementation. This culminated in the creation of a geo-graphic map delineating the zones of probability distribution, as presented in Figure 4.

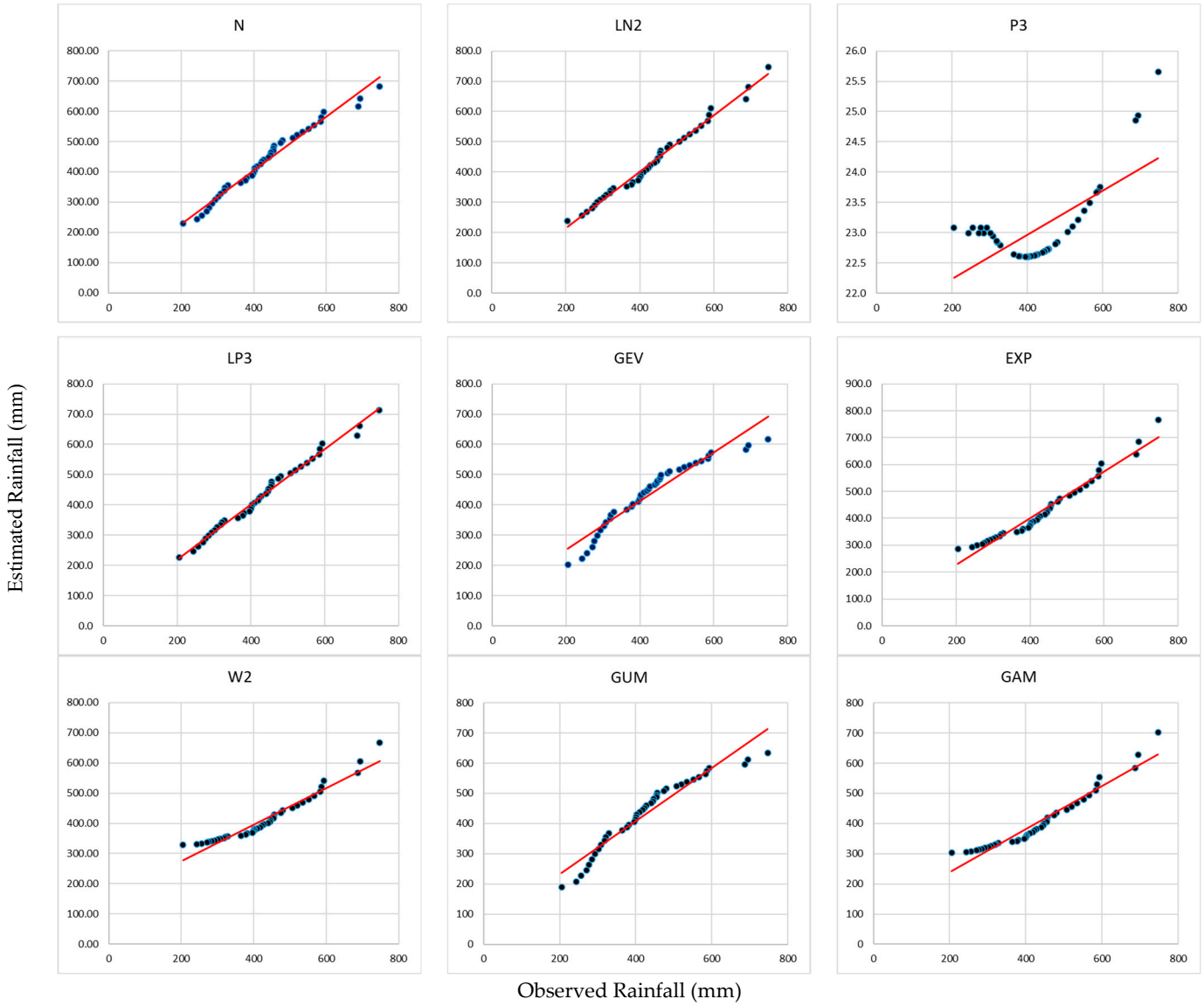

Figure 3. Q-Q plot of all distribution at a district of Punjab: Lahore.

The probability zoning map for Pakistan, developed through a comprehensive analysis of historical rainfall data, offers valuable insights into the spatial distribution of rainfall probability distributions across the country. The analysis involved the assessment of nine different probability distributions, revealing that five of these distributions—log Pearson, Weibull, log normal, Generalized Extreme Value, and gamma—emerged as the best-fit models for various districts in Pakistan. The details regarding the developed probabilistic zones of rainfall distribution for Pakistan has been provided in Table 3. The tabular data show all the districts along with their area coverage for the five best-fit probability distributions, based on the analysis. The names of the provinces have also been mentioned to provide a better understanding of the location of the districts and their probabilistic zone categorization.

Table 3. Details regarding the probabilistic zones for rainfall data for Pakistan.

GEV			LP3			LN2		
Province	**District Name**	**Area (km^2)**	**Province**	**District Name**	**Area (km^2)**	**Province**	**District Name**	**Area (km^2)**
Gilgit-Baltistan	Astore	8657	Khyber Pakhtunkhwa	Hangu	1097	Balochistan	Sherani	4310
	Diamer	7340		Kohat	2991		Musakhel	5728
	Ghanche	6400		North Waziristan	4707		Zhob	15,987
	Ghizer	9612		South Waziristan	5434		Loralai	3785
	Gilgit	3800		Lakki Marwat	3296		Dukki	4233
	Hunza	7430		Bannu	1972		Barkhan	3514
	Kharmang	5500		Karak	3371	Punjab	Bhakkar	8153
	Nagar	5000		Kurram	3380		Layyah	6289
	Shigar	8500		Khyber	2576		Khushab	6511
	Skardu	10,732		Orakzai	1538		Jhang	6166
Khyber Pakhtunkhwa	Mardan	1632		Charsadda	996		Chakwal	6525
	Mansehra	4125		Buner	1865		Gujranwala	3622
	Malakand	8041		Bajaur	1290		Hafizabad	2367
	Dir	5282		Peshawar	1518		NankanaSahib	2216
	Swat	5337		Nowshera	1748		Lahore	1772
	Shangla	1586		Swabi	1543		Khanewal	4349
	Battagram	1301	Punjab	Attock	6857		Muzaffargarh	8249
	Kohistan	2043		Islamabad	2642		DeraGhaziKhan	11,922
	Chitral	14,850		Rawalpindi	5285		Multan	3720
GAM				Mianwali	5840		Lodhran	2778
Province	**District Name**	**Area (km^2)**		Jhelum	3587		Bahawalnagar	8878
Punjab	Okara	4377		Gujrat	3192		Bahawalpur	24,830
	Sahiwal	3201		Mandi Bahauddin	2673		RahimYarKhan	11,880
	TobaTekSingh	3252		Sialkot	3016	Sindh	Ghotki	6083
	Vehari	4364	Balochistan	Qilla Safiullah	6831		Shikarpur	2512
	Pakpattan	2724		Ziarat	3301		Sukkur	5165
	Narowal	2337		Pishin	6218		Mirpurkhas	2925
	Sargodha	5856		Chaman	1341		Tando Allahyar	1554
	Faisalabad	5857		Qilla Abdullah	3553		Sanghar	10,728
	Sheikhupura	3744		Quetta	3447		Khairpur	15,910
	Kasur	3995		Mastung	3308	Khyber Pakhtunkhwa	Mohmand	2296
Sindh	Jamshoro	11,260		Kalat	7654		Abbottabad	1967
	Karachi	3527		Nushki	5797		Haripur	1725
	Thatta	8570		Kharan	14,958	**W2**		
	Badin	6858		Surab	762	**Province**	**District Name**	**Area (km^2)**
	Tharparkar	19,637		Chagai	44,748	Balochistan	Harnai	2492
	Umarkot	5608		Washuk	33,093		Kachhi	12,398
	Tando M. Khan	1778		Panjgur	16,891		Khuzdar	35,380
	Hyderabad	9077		Kech	22,539		Jhal Magsi	3615
Khyber Pakhtunkhwa	Tank	2900		Gwadar	12,637		Kohlu	7610
	Dera Ismail Khan	9334	Sindh	Qambar Shahdatkot	5475		Sibi	7121
				Jacobabad	2686		Dera Bugti	10,160
				Larkana	1948		Nasirabad	3387
				Matiari	1717		Jafarabad	1643
				Dadu	7856		Sohbatpur	802
				Naushahro Feroze	2946		Awaran	29,510
							Lasbela	8437
						Sindh	Kashmore	2592
							Shaheed Benazirabad	4502
						Punjab	Rajanpur	12,318

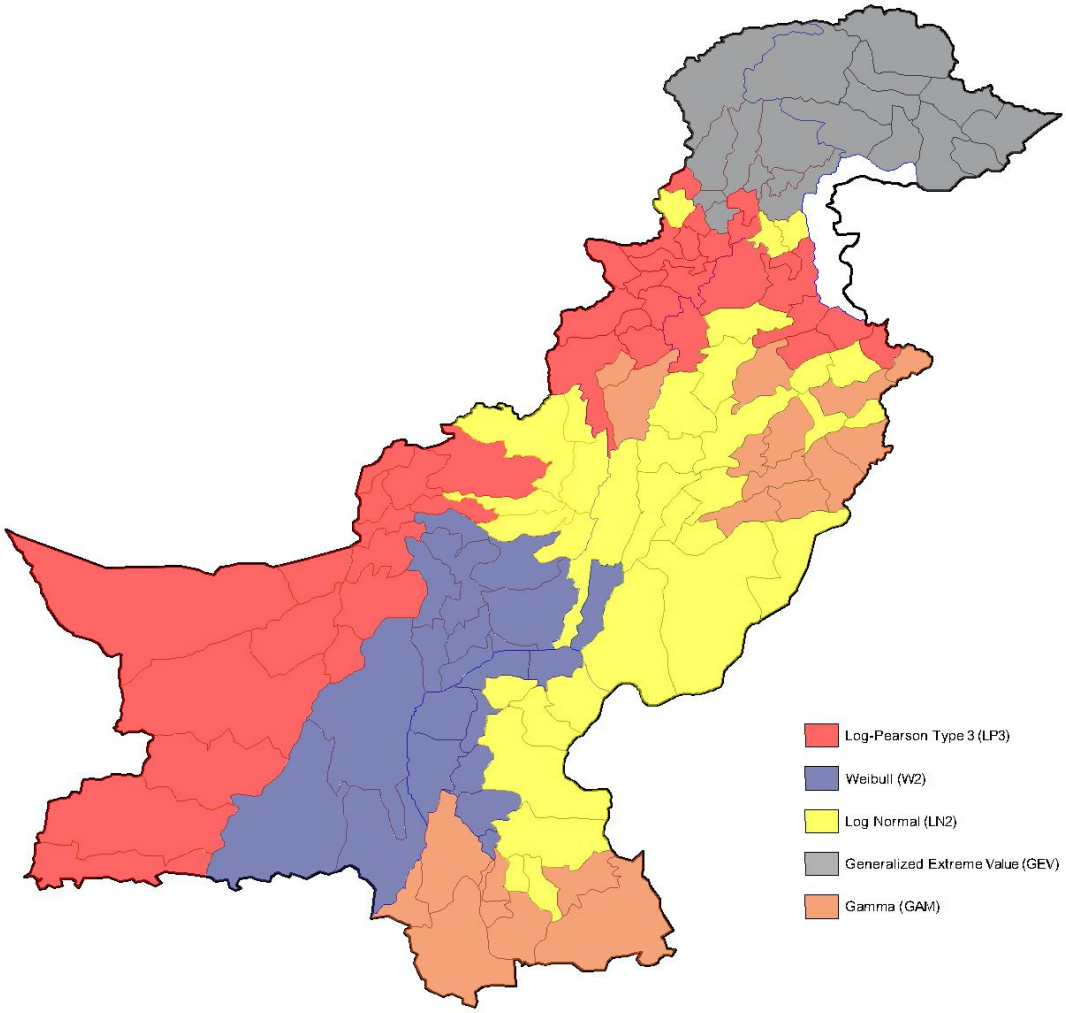

Figure 4. Probabilistic zoning map of rainfall data for Pakistan.

Provincially, the distribution patterns exhibit distinctive characteristics. In Punjab, the central and southern regions are dominated by the log normal distribution, while the northeastern areas, including districts like Mandi Bahauddin and Sialkot, show a preference for LP3. In Sindh, a diverse distribution emerges, with GAM and LN2 covering approximately 40% of districts each. GAM prevails along the southern coast, including districts such as Karachi and Thatta, while LN2 is prominent in the northeast, encompassing areas like Khairpur and Sukkur. W2 claims its place on the northwestern side, including districts like Larkana and Dadu. Balochistan's districts exhibit a mix of LP3, W2, and LN2 distributions. LP3 dominates the western side of the province, encompassing regions like Washuk and Panjgur, while W2 prevails in the east, connecting with Sindh. LN2 takes charge of the northern part, connecting with Punjab and Khyber Pakhtunkhwa. In Khyber Pakhtunkhwa (KPK), GEV and LP3 are the dominant distributions, with GEV prominent in the northern high-altitude areas, including Chitral and Swat. LP3 prevails in the middle and southeastern regions, covering districts like Kohat and Kurram. A small section of GAM appears in the southeastern part, connecting with Punjab. The Gilgit-Baltistan region stands out with its exclusive dominance of the GEV distribution, which is well-suited to its high-altitude and cold-temperate environment. This comprehensive analysis of the probability distributions in the provinces has been summarized visually in Figure 5.

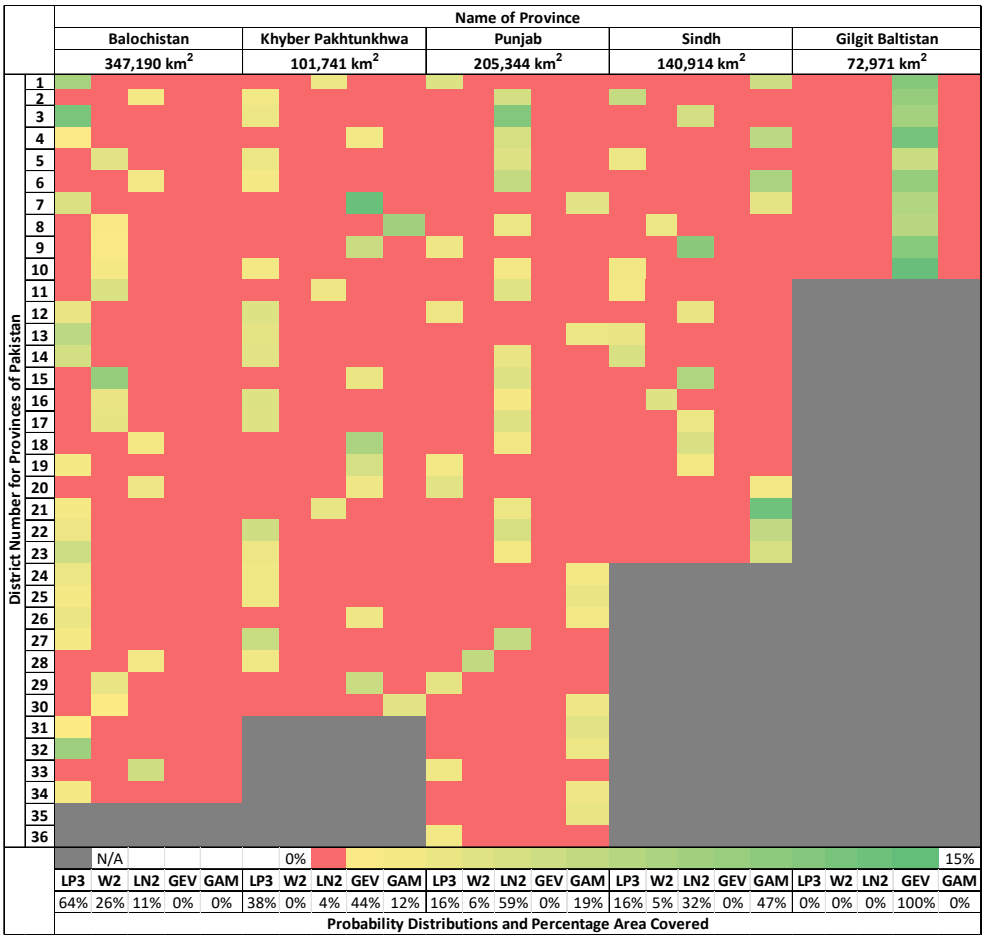

Figure 5. Heat map for area covered by probability distributions in Provinces of Pakistan.

The developed zones can now be correlated with the climatic zones and topography of the region under consideration. Utilizing the available information regarding the climatic zones of Pakistan and the newly developed rainfall probabilistic zones, a detailed comparison and analysis was carried out, which has been summarized in Table 4, as shown. It can be noted that a set of distributions fall within a climatic zone, however, one of the distributions is dominating the zone. Using the defined geological features and characteristics of the zones, certain correlations can be developed.

As discussed earlier, the climatic Zone-A has a mountainous topography as well as a very cold climate. The GEV distribution is dominant in that region, which validates that, with these geographical and climatic features, GEV distribution is the most well suited. Similarly, Zone-B has moderately hilly topographical features with a comparatively mild cold climate and frequent rainfall, which is appropriately described by the LP3 distribution that dominates in this region, followed by LN2. Zone-C also has a clear dominance of LP3, confirming the hilly features and extreme climate conditions in different seasons. Zone-D reflects LN2 followed by W2 distribution, indicating the hot and dry region of the country, with low annual rainfall and frequent droughts. Zone-E is mainly represented by GAM, which indicates the existence of an arid climate in the zone, along with humidity and warm temperatures due to the coast.

Beyond provincial divisions, the map underscores the correlation between rainfall probability distributions and the geographical and climatic characteristics. The analysis was carried out by plotting a heat map for the spatial coverage of best-fit probability distributions in the climatic zones of Pakistan, as shown in Figure 6.

Table 4. Districts within the climatic zones of Pakistan and their corresponding best-fit rainfall distributions.

Climate Zone—A			Climate Zone—B			Climate Zone—C		
Province	**District Name**	**Best-Fit Distribution**	**Province**	**District Name**	**Best-Fit Distribution**	**Province**	**District Name**	**Best-Fit Distribution**
Gilgit-Baltistan	Astore	GEV	Khyber Pakhtunkhwa	Hangu	LP3	Balochistan	Sherani	LN2
	Diamer	GEV		Kohat	LP3		Musakhel	LN2
	Ghanche	GEV		North Waziristan	LP3		Zhob	LN2
	Ghizer	GEV		South Waziristan	LP3		Qilla Safiullah	LP3
	Gilgit	GEV		Tank	GAM		Loralai	LN2
	Hunza	GEV		Dera Ismail Khan	GAM		Dukki	LN2
	Kharmang	GEV		Lakki Marwat	LP3		Ziarat	LP3
	Nagar	GEV		Bannu	LP3		Pishin	LP3
	Shigar	GEV		Karak	LP3		Chaman	LP3
	Skardu	GEV	Punjab	Attock	LP3		Qilla Abdullah	LP3
Khyber Pakhtunkhwa	Kurram	LP3		Islamabad	LP3		Quetta	LP3
	Khyber	LP3		Rawalpindi	LP3		Harnai	W2
	Orakzai	LP3		Mianwali	LP3		Mastung	LP3
	Mohmand	LN2		Bhakkar	LN2		Kachhi	W2
	Charsadda	LP3		Layyah	LN2		Kalat	LP3
	Mardan	GEV		Khushab	LN2		Nushki	LP3
	Buner	LP3		Jhang	LN2		Kharan	LP3
	Mansehra	GEV		Chakwal	LN2		Surab	LP3
	Bajaur	LP3		Jhelum	LP3		Khuzdar	W2
	Malakand	GEV		Gujrat	LP3		Jhal Magsi	W2
	Dir	GEV		Mandi Bahauddin	LP3	Sindh	Qambar Shahdatkot	LP3
	Swat	GEV		Sialkot	LP3			
	Shangla	GEV		Narowal	GAM			
	Battagram	GEV		Gujranwala	LN2			
	Kohistan	GEV		Hafizabad	LN2			
	Chitral	GEV		Sargodha	GAM			
	Abbottabad	LN2		Faisalabad	GAM			
	Peshawar	LP3		NankanaSahib	LN2			
	Nowshera	LP3		Sheikhupura	GAM			
	Swabi	LP3		Lahore	LN2			
	Haripur	LN2		Kasur	GAM			

Climate Zone—D			Climate Zone—E		
Province	**District Name**	**Best-Fit Distribution**	**Province**	**District Name**	**Best-Fit Distribution**
Punjab	Okara	GAM	Balochistan	Chagai	LP3
	Sahiwal	GAM		Washuk	LP3
	TobaTekSingh	GAM		Panjgur	LP3
	Khanewal	LN2		Kech	LP3
	Muzaffargarh	LN2		Gwadar	LP3
	DeraGhaziKhan	LN2		Awaran	W2
	Multan	LN2		Lasbela	W2
	Lodhran	LN2	Sindh	Dadu	LP3
	Vehari	GAM		Naushahro Feroze	LP3
	Pakpattan	GAM		Shaheed Benazirabad	W2
	Bahawalnagar	LN2		Jamshoro	GAM
	Bahawalpur	LN2		Karachi	GAM
	RahimYarKhan	LN2		Thatta	GAM
	Rajanpur	W2		Badin	GAM
Balochistan	Barkhan	LN2		Tharparkar	GAM
	Kohlu	W2		Umarkot	GAM
	Sibi	W2		Mirpurkhas	LN2
	Dera Bugti	W2		Tando Allahyar	LN2
	Nasirabad	W2		Tando M. Khan	GAM
	Jafarabad	W2		Hyderabad	GAM
	Sohbatpur	W2		Matiari	LP3
Sindh	Ghotki	LN2		Sanghar	LN2
	Kashmore	W2		Khairpur	LN2
	Jacobabad	LP3			
	Shikarpur	LN2			
	Larkana	LP3			
	Sukkur	LN2			

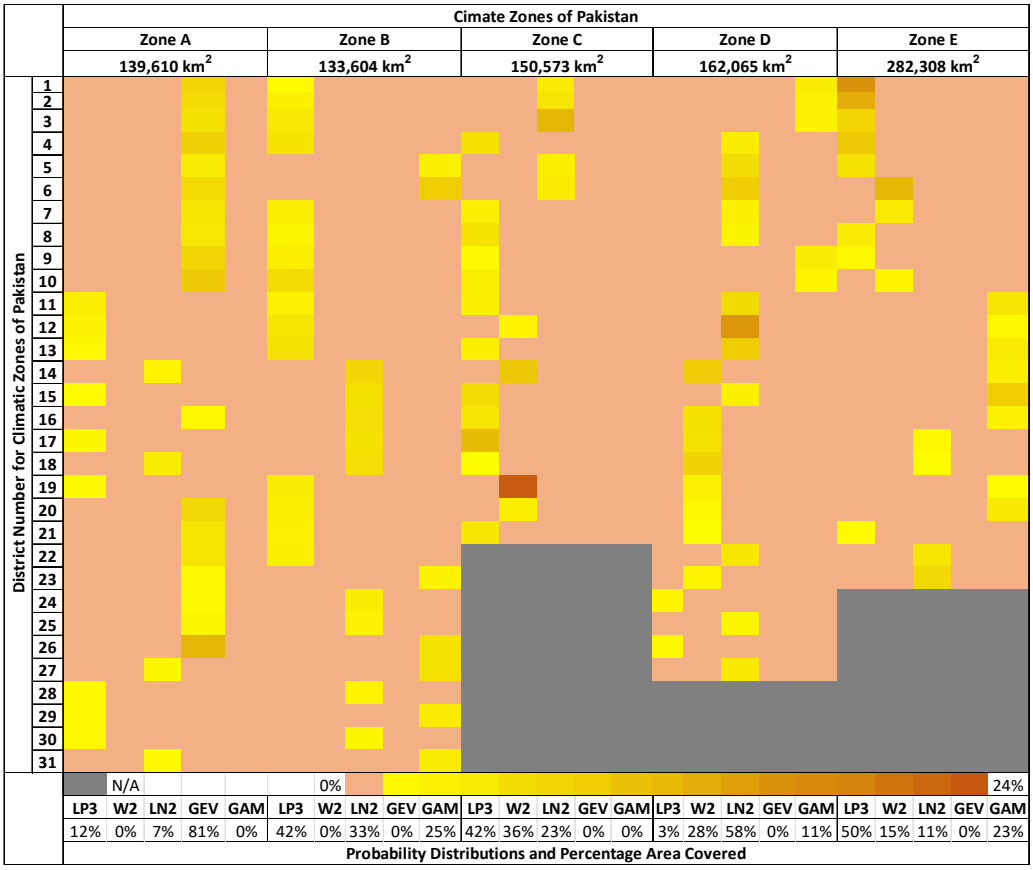

Figure 6. Heat map for area covered by probability distributions in climatic zones of Pakistan.

Figure 6 is helpful in generating valuable insights about the spatial allocation of probability distributions with respect to the climatic zones of the region, as defined by PMD. From the figure, it can be noted that GEV is mainly associated with the northern, high-altitude regions (Zone-A), while LP3 extends its dominance into mountainous areas with varying temperature conditions. W2 claims territory along the Indus River, particularly downstream from Panjnad, making it highly susceptible to flooding. GAM finds its stronghold in the coastal regions of Sindh (Zone-E), while LN2 prevails in the plains, deserts, and high-temperature zones (Zone-D). Additionally, GAM is noticeable in slightly hilly areas.

This probability zoning map not only enhances our understanding of the rainfall distribution across Pakistan but also provides a valuable tool for decision-makers in various sectors, including agriculture and water resource management, so that they can determine the frequency of extreme rainfall events in any location across the region, enabling them to make more informed choices based on the distinct rainfall characteristics of each region. The probabilistic modeling in this study will ease area identification for regions with high vulnerability to hazardous extreme events. It will provide insights for the formation of streamlined mitigation strategies and effective resource allocation for the entire study region.

3.2. Return Period Results

Figure 7 illustrates the precipitation return values across all districts within the region at intervals of 10, 25, 50, and 100 years. The Figure's horizontal axis corresponds to the district numbers, as indicated in Table 1, while the vertical axis represents the maximum monthly rainfall. This graphical representation is divided into four distinct segments, each corresponding to a specific return period of 10, 25, 50, or 100 years. Notably, Figure 7

provides a visual depiction of the return values based on the best-fitting probability distribution for each district in the region. For example, for the Islamabad district (district 36), which is best fitted by the LP3 distribution, as seen in Figure 7c, the maximum monthly rainfall levels are observed to be 86.9 mm, 104.4 mm, 122 mm, and 158.6 mm for the return periods of 10, 25, 50, and 100 years, respectively.

The primary objective behind generating the return period results lies in facilitating informed decision-making and the formulation of effective mitigation strategies by the relevant governing authorities. This process hinges on a comprehensive analysis enriched with empirical evidence, thereby ensuring that ongoing decision-making processes are substantiated and carry substantial impact. To illustrate, let us consider the case of Islamabad. A risk assessment plan, rooted in the LP3 distribution over a 50-year timeframe, can be meticulously crafted. This plan plays a pivotal role in forecasting the anticipated average maximum monthly rainfall, which, in this instance, stands at 122 mm. This estimation boasts a remarkable 95% confidence level, encompassing a range from 97.6 mm to 146.9 mm. Armed with this critical data, a well-structured risk mitigation strategy can be devised to pre-emptively manage potential hazards before they manifest into actual events, thereby averting substantial damages and ensuring resilient disaster preparedness.

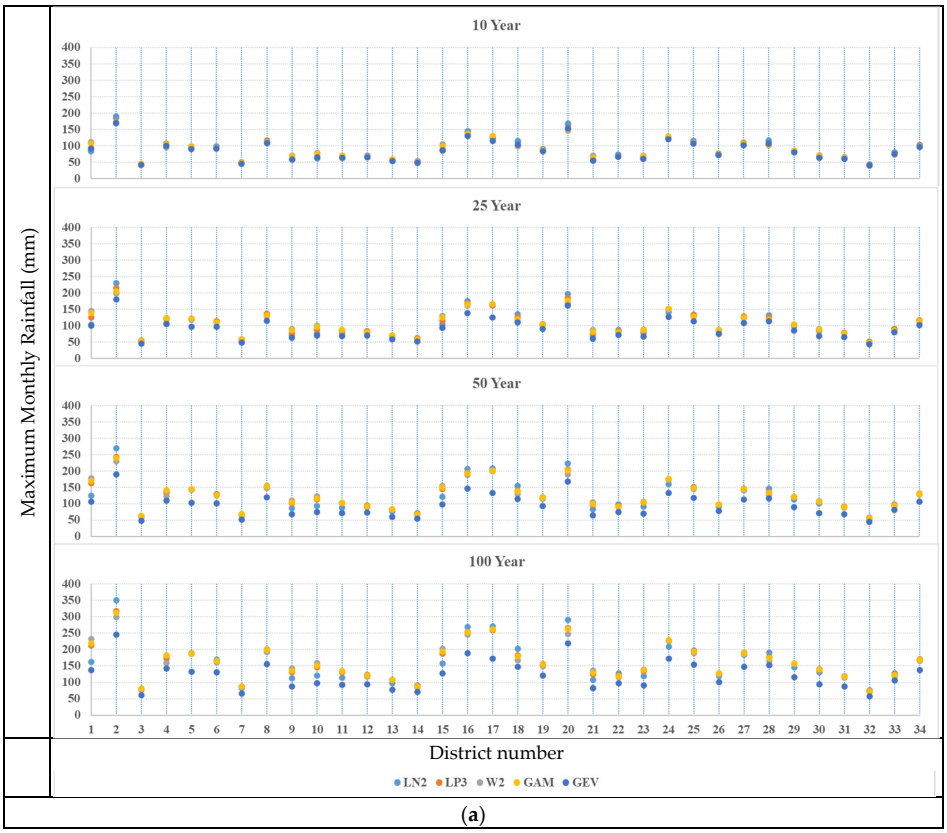

Figure 7. *Cont.*

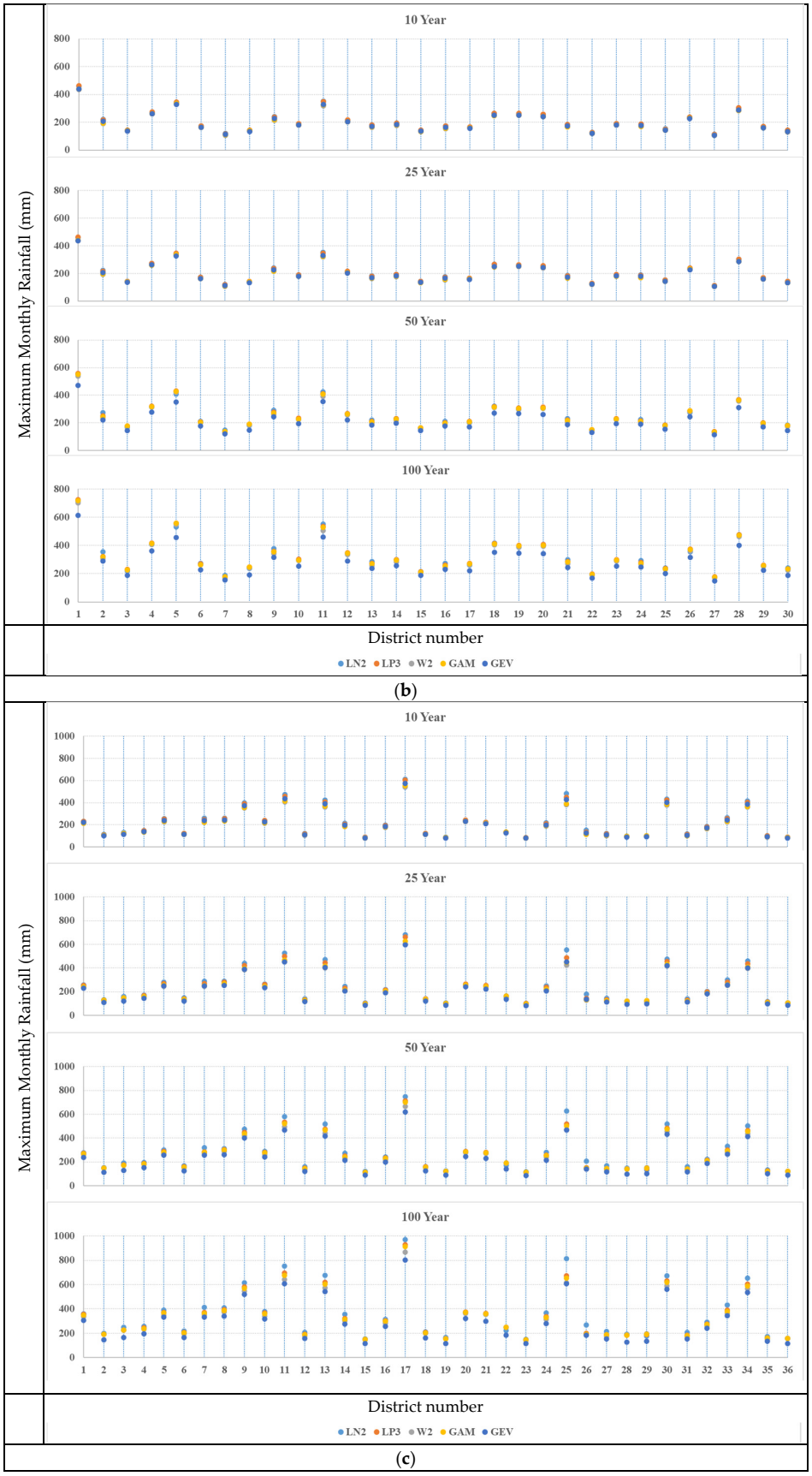

Figure 7. *Cont.*

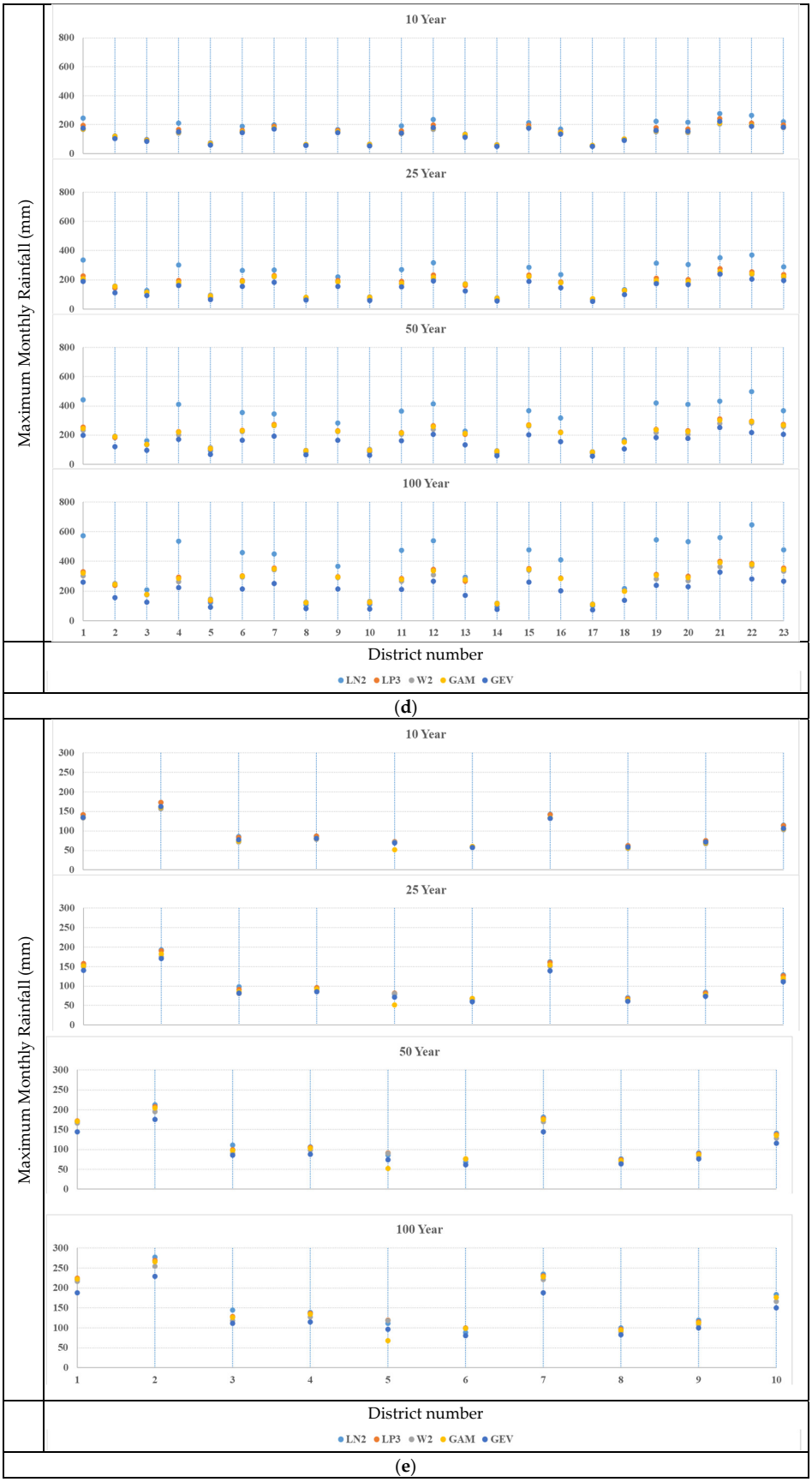

Figure 7. (**a**) Return period results for all districts of Balochistan. (**b**) Return period results for all districts of Khyber Pakhtunkhwa. (**c**) Return period results for all districts of Punjab. (**d**) Return period results for all districts of Sindh. (**e**) Return period results for all districts of Gilgit-Baltistan.

4. Discussion

This study thoroughly explores the complex realm of rainfall probability distribution modeling, a crucial aspect of hydro-climatology and flood risk assessment. The analysis covered a diverse and geographically extensive region, where the complexities of rainfall patterns and their implications for disaster management are of paramount importance.

Estimating the expected rainfall values in different timeframes, whether they are higher or lower than what has been recorded, is carried out by fitting a probability distribution model to the data. Accurate predictions of extreme rainfall can help to minimize storm damage and improve the design of water management infrastructure.

The fundamental significance of this research lies in the development of a novel probabilistic zoning map, an innovation that has hitherto been absent in the scientific discourse. The investigation provided significant insights into the spatial distribution of rainfall occurrences in the region by using a range of probability distributions, including log Pearson type-III, Weibull, log normal, Generalized Extreme Value, and gamma distributions. Frequency analysis was conducted on the precipitation data from all districts across the provinces of Pakistan to identify their best-fit probability distributions and create probabilistic zones. Various researchers around the world have studied smaller regions or basins to determine one best-fit probability distribution for that complete region or basin under study [61–70] but the concept of the probabilistic zoning map developed in this study considers the diverse characteristics and variations within a larger region, providing a more comprehensive and accurate representation of rainfall patterns. Nassif et al. used the monthly rainfall data for fourteen stations in Iraq to determine the suitable probability distribution for these regions, but the research did not conclude any best-fit distribution that could be applied to the cities/regions under consideration as the considered goodness-of-fit tests did not provide a consistent conclusion [61]. Similarly, Ng et al. investigated the best-fit distribution for the Kelantan River Basin using observational data from established weather stations in the basin and concluded that GEV was the best-fit distribution for the basin [63]. However, one of the stations indicated LP3 as its best fit. From this, it can be noted that an entire basin or study region cannot be defined with just one probability distribution. Subsequently, in this research, probabilistic zones were developed, highlighting the hotspot regions for various distributions under consideration for the entire country of Pakistan.

To determine the best-fit distribution for each district across the provinces of Pakistan, goodness-of-fit tests were conducted, including the Kolmogorov–Smirnov, Anderson–Darling, and root mean squared error [66,71,72]. These tests have played a pivotal role in guiding the ranking method used in this research to determine the best-fit probability distribution for the districts and then in the development of the zoning map. The test statistic values have been the deciding parameter for the best-fit distribution selection, a concept adopted recently by various researchers [63,66]. Consequently, the findings of this study can serve as a valuable resource for government departments and relevant authorities involved in flood risk management, water resource management, and disaster preparedness in highly vulnerable subregions of Pakistan.

The results are both enlightening and transformative. The study confirms that the selection of probability distribution is closely linked to geographical and climatic attributes [73–75]. Walha et al. has discussed a linkage when investigating rainfall variations in Punjab province and their effects on the agricultural production and provincial economy [5]. Climatic zones and variations are closely linked to the rainfall distribution of the region under consideration. Developing appropriate zoning maps can assist in addressing the concerns in a region based on its vulnerability. Identifying the distribution zone from the map can help in managing the cropping patterns and strategic agricultural

planning based on water availability and flood frequency due to heavy rainfall. The crop production in the region may then be planned accordingly.

By identifying the most appropriate probability distributions for each district, this research enhances the accuracy of flood risk assessment and disaster management strategies [76,77]. Khan et al. have identified that the frequency of occurrence of extreme events is increasing in Pakistan, which is affecting the agricultural productivity, preservation of water resources, and hydraulic infrastructure [47]. Therefore, determining the best-fit probability distribution is of immense importance to water resource management and strategic planning of resources. The log normal distribution is prevalent in Punjab, indicating the distinct climatic conditions of the central and southern regions, an indication of which was available through recent research by Wahla et al. and Reggiani et al. [5,78].

The distribution of rainfall in Sindh varies across different areas, with GAM, LN2, and W2 dominating specific regions. Coastal areas are mainly characterized by GAM, while the northeastern regions are known for LN2 [3,79]. In the northwestern districts, W2 plays a significant role in determining the rainfall pattern. This distribution is affected by both coastal positioning and the arid expanse to the northeast [80]. This linkage was highlighted by Ahmed et al. when evaluating gridded rainfall over arid regions of Pakistan. This finding was supported by the conclusions given in the corresponding research based on the hydro-climatological studies of the ungauged arid regions. Utilizing satellite-based dataset such as CHRIPS can eliminate the difficulty of obtaining observed data for such regions. The suitability and accuracy of CHIRPS has already been established, ensuring its application for rainfall analysis.

Balochistan has a diverse range of geological and climatic characteristics. LP3 dominates the western side, while W2 prevails in the east, connecting with Sindh through its varied terrain [81–83]. These findings highlight the need for localized and tailored approaches to flood risk management, considering the unique rainfall patterns and characteristics of each district. Khyber Pakhtunkhwa's districts show a clear pattern based on geographical differences. In Khyber Pakhtunkhwa, the dominant distributions are GEV and LP3, with GEV prominent in the northern high-altitude areas [84]. LP3 prevails in the middle and southeastern regions, including district [85]. A small section of GAM is present in the southeastern part, connecting with Punjab. The region of Gilgit-Baltistan is characterized by a significant prevalence of the Generalized Extreme Value distribution, which is specifically suitable for its cold-temperate and high-altitude environment [86,87]. These findings shed light on the complex relationship between rainfall patterns and geographical/climatic attributes, providing valuable insights for effective flood risk management and disaster preparedness.

This innovative probabilistic zoning map, resulting from this thorough analysis, offers valuable insights for a range of stakeholders such as government entities, disaster management agencies, and policymakers. The identification of the most suitable probability distribution for each region serves as a critical foundation for developing tailored risk assessment and mitigation strategies, which are essential for effective decision-making and planning. It empowers decision-makers to predict rainfall extremes with enhanced accuracy and, consequently, to institute pre-emptive measures to safeguard lives, infrastructure, and livelihoods. For instance, the zoning map can guide the placement of essential flood-control hydraulic structures and early warning systems. The LN2 region specified in the map is the most vulnerable to extreme rainfall events and flooding, as per the detailed analysis conducted in this research, followed by GAM, LP3, W2, and then GEV. Therefore, the strategic planning for installation of early warning systems in the entire country will prove to be highly effective if the most vulnerable region (LN2), as per the zoning map, is prioritized in the process. The same sequence may then be followed as a continuation, as

per the degree of vulnerability of the other zones in the region. In this way, the probabilistic zoning map can be utilized to make informed decisions in planning and mitigation of extreme events.

The developed map can assist in planning quick response roadmaps for areas subject to extremely high-intensity precipitation, based on the frequency and intensity of rainfall in the region as well as its degree of vulnerability. Likewise, the insights gained from this study can assist the development of sustainable agricultural practices and water conservation, particularly in regions with a higher likelihood of droughts or floods [47]. The comprehensive rainfall analysis in this study and the prepared zoning map can contribute to the enhancement of urban resilience, empowering urban planners to develop effective stormwater management systems and ensure the protection of critical infrastructure. Considering the degree of vulnerability of an area from the zoning map of the entire region, the findings from this study would be useful to urban planners and government officials to allow them to make informed decisions on urban development to benefit the community, especially those living in areas at risk from flash flooding from heavy rain events.

The current capability of the meteorological department is limited in various aspects and needs to be developed. The forecasting range is just a few days, which is not sufficient for a developing country like Pakistan, where resources are limited. The department lacks a detailed quantitative prediction mechanism for extreme events, which was one of the reasons behind the 2010 and 2014 floods in Pakistan. There is a deficiency of atmospheric data and, due to this, there is difficulty observing and tracking storms. There is no well-established urban flood-forecasting system except the one located in Islamabad.

A significant and far-reaching outcome of this research endeavor lies in the comprehensive estimation of return periods, considering all districts across the region and the diverse distributions prevailing throughout Pakistan. The inclusive portrayal of these distributions provides a holistic assessment of the spectrum of anticipated return periods, highlighting the most probable outcome, which aligns with the best-fit distribution [3,47,79]. Precipitation return values were meticulously computed for varying time horizons, spanning 10, 25, 50, and 100 years. Notably, the results for the 100-year return period, while exceptionally impactful, are characterized by their rarity, presenting an inverse relationship when compared to the findings for the 10-year return period [79,88]. These insights carry profound implications for decision-makers, who must navigate the intricacies of risk management, encompassing considerations of both the duration and severity of potential events.

The findings of this study hold significant practical implications. Based on the insights from the study, the following recommendations are proposed:

- The probabilistic zoning map may be considered as an efficient tool for an integrated disaster management framework. A collaboration of the local as well as the national authorities can prove to be beneficial by developing and implementing region-specific strategies that can help mitigate the impacts of extreme rainfall events.
- The environmental conditions affect the climate and geography of a region. As we are connected to our neighboring riparian countries, an efficient transboundary information exchange can help identify and overcome the deficiencies in the system.
- Establishing a district-level disaster management system can enhance the effectiveness of monitoring and early warning processes. With the help of identified best-fit probability distributions, as determined in this study, the flood-forecasting process for urban and flood-prone areas can be improved.
- Local-level risk assessment can prove to be effective in terms of resource allocation, development initiatives, and land-use planning.
- Establishing a well-maintained network of weather monitoring stations will improve the precision of rainfall data. This will be very useful for the underserved areas.

- It would be beneficial if the disaster management systems were to reduce their dependance on field observational data and instead make use of satellite-based data for easy, quick, and accurate analysis of data.
- Effective communication and community engagement are pivotal. Public awareness campaigns can educate vulnerable populations about the risks associated with extreme rainfall events and the importance of preparedness.
- This study paves the way for future research endeavors. Long-term monitoring of rainfall patterns, investigating the influence of climate change, and refining the probability distributions merit ongoing research investigation.

5. Conclusions

Selecting an appropriate probability distribution model is vital for predicting extreme rainfall in arid and semi-arid regions, particularly in countries with diverse climatic conditions. This study evaluated and assessed various probability distributions for the rainfall datasets and developed a probabilistic zoning map to enhance risk assessment and storm impact mitigation. The zoning map provides a foundation for planning strategies in water resource management, disaster preparedness, and also planning for flood resilience. Spatial analysis revealed that LN2 dominated central and southern Punjab, GAM prevailed in coastal Sindh, and Balochistan displayed a mix of W2, LP3, and LN2. GEV was exclusive to mountainous Gilgit-Baltistan, while Khyber Pakhtunkhwa featured GEV and LP3. Distinct patterns emerged: GEV dominated high-altitude, cold-temperate areas; LP3 was typical in variable-temperature mountainous regions; and W2 was common along the flood-prone Indus River. The probabilistic zoning map, based on thorough analysis, provides Pakistan with an effective tool to deal with the challenges of climate variability and disaster risk management. Moreover, comprehending the pattern of heavy rainfall will be crucial in multiple sectors, particularly when implementing measures for ecological balance and supporting Pakistan's vital agriculture industry—a cornerstone of the nation's GDP. Implementing these findings can contribute to a more secure and robust future for the country amidst increasingly erratic weather patterns. By understanding the probability distribution of rainfall in different regions of Pakistan, policymakers and planners can make informed decisions regarding land use, infrastructure development, and disaster preparedness, ultimately leading to enhanced resilience and better allocation of resources.

Author Contributions: Conceptualization, F.H. and S.A.; data curation, F.H. and N.A. (Naveed Ahmed); formal analysis, S.A., N.A. (Naveed Ahmed), N.A. (Nassir Alarifi), and Y.M.Y.; funding acquisition, N.A. (Nassir Alarifi); investigation, S.A.; methodology, F.H. and S.A.; project administration, N.A. (Nassir Alarifi); resources, N.A. (Nassir Alarifi); software, F.H. and Y.M.Y.; supervision, S.A.; validation, N.A. (Naveed Ahmed) and Y.M.Y.; visualization, Y.M.Y.; writing—original draft, F.H., S.A. and N.A. (Naveed Ahmed); and writing—review and editing, N.A. (Nassir Alarifi) and Y.M.Y. All authors have read and agreed to the published version of the manuscript.

Funding: This research received no external funding.

Institutional Review Board Statement: Not applicable.

Informed Consent Statement: Not applicable.

Data Availability Statement: The original contributions presented in the study are included in the article; further inquiries can be directed to the corresponding author.

Acknowledgments: This research was supported by the Researchers Supporting Project number (RSPD2025R804), King Saud University, Riyadh, Saudi Arabia. The authors are also grateful to the National University of Computer and Emerging Sciences (NUCES) for providing the required

facilities. It is acknowledged that all authors have reviewed. We are also thankful to the Pakistan Meteorological Department (PMD) for providing the data for this research.

Conflicts of Interest: The authors declare no conflicts of interest.

References

1. Katz, R.W.; Brown, B.G. Extreme events in a changing climate: Variability is more important than averages. *Clim. Chang.* **1992**, *21*, 289–302. [CrossRef]
2. Stedinger, J. Fitting Log Normal Distributions. *Water Resour. Res.* **1980**, *16*, 481–490. [CrossRef]
3. Ali, G.; Sajjad, M.; Kanwal, S.; Xiao, T.; Khalid, S.; Shoaib, F.; Gul, H.N. Spatial-temporal characterization of rainfall in Pakistan during the past half-century (1961–2020). *Sci. Rep.* **2021**, *11*, 6935. [CrossRef]
4. Ahmed, K.; Shahid, S.; Chung, E.S.; Ismail, T.; Wang, X.J. Spatial distribution of secular trends in annual and seasonal precipitation over Pakistan. *Clim. Res.* **2017**, *74*, 95–107. [CrossRef]
5. Wahla, S.S.; Shirazi, S.A.; Abbas, S.; Hussain, M.S.; Khurshid, M. Seasonal and regional variations in rainfall distribution over the Punjab-Pakistan. *Int. J. Econ. Environ. Geol.* **2020**, *10*, 109–114.
6. The Government of Pakistan; Asian Development Bank; European Union; United Nations Development Programme; World Bank. Published by Ministry of Planning Development & Special Initiatives, Islamabad, Pakistan. Pakistan Floods 2022—Post Disaster Needs Assessment. Main Report. 2022. Available online: https://www.undp.org/pakistan/publications/pakistan-floods-2022-post-disaster-needs-assessment-pdna (accessed on 7 October 2024).
7. Zomer, R.J.; Xu, J.; Trabucco, A. Version 3 of the Global Aridity Index and Potential Evapotranspiration Database. *Sci. Data* **2022**, *9*, 409. [CrossRef]
8. Subudhi, R. Probability analysis for prediction of annual maximum daily rainfall of Chakapada block of Kandhamal district in Orissa. *Indian J. Soil Conserv.* **2007**, *35*, 84–85.
9. Bhakar, S.R.; Iqbal, M.; Devanda, M.; Chhajed, N.; Bansal, A.K. Probability analysis of rainfall at Kota. *Indian J. Agri. Res.* **2008**, *42*, 201–206.
10. Tao, D.Q.; Nguyen, V.T.; Bourque, A. On selection of probability distributions for representing extreme precipitations in Southern Quebec. In Proceedings of the Annual Conference of the Canadian Society for Civil Engineering, Montreal, QC, Canada, 5–8 June 2002; pp. 1–8.
11. Upadhaya, A.; Singh, S.R. Estimation of consecutive day's maximum rainfall by various methods and their comparison. *Indian J. Soil Conserv.* **1998**, *26*, 193–201.
12. Bhakar, S.R.; Bansal, A.N.; Chhajed, N.; Purohit, R.C. Frequency analysis of consecutive days maximum rainfall at Banswara, Rajasthan, India. *ARPN J. Eng. Appl. Sci.* **2006**, *1*, 64–67.
13. Mandal, S.; Choudhury, B.U. Estimation and prediction of maximum daily rainfall at Sagar Island using best fit probability models. *Theor. Appl. Clim.* **2015**, *121*, 87–97. [CrossRef]
14. Kumar, A. Prediction of annual maximum daily rainfall of Ranichauri (Tehri Garhwal) based on probability analysis. *Indian J. Soil Conserv.* **2000**, *28*, 178–180.
15. Singh, R.K. Probability analysis for prediction of annual maximum rainfall of Eastern Himalaya (Sikkim mid hills). *Indian J. Soil Conserv.* **2001**, *29*, 263–265.
16. Amin, M.; Rizwan, M.; Alazba, P. A best-fit probability distribution for the estimation of rainfall in northern regions of Pakistan. *Open Life Sci.* **2016**, *11*, 432–440. [CrossRef]
17. Eslamian, S.S.; Feizi, H. Maximum Monthly Rainfall Analysis Using L-Moments for an Arid Region in Isfahan Province, Iran. *J. Appl. Meteorol. Climatol.* **2007**, *46*, 494–503. [CrossRef]
18. Lee, C. Application of rainfall frequency analysis on studying rainfall distribution characteristics of Chia-Nan plain area in Southern Taiwan. *Crop Environ. Bioinf.* **2005**, *2*, 31–38.
19. Ogunlela, A.O. Stochastic Analysis of Rainfall Evens in Ilorin, Nigeria. *J. Agric. Res. Dev.* **2001**, *1*, 39–50.
20. Kwaku, X.S.; Duke, O. Characterization and frequency analysis of one day annual maximum and two to five consecutive days maximum rainfall of Accra, Ghana. *ARPN J. Eng. Appl. Sci.* **2007**, *2*, 27–31.
21. Olofintoye, O.O.; Sule, B.F.; Salami, A.W. Best fit Probability distribution model for peak daily rainfall of selected Cities in Nigeria. *N. Y. Sci. J.* **2009**, *2*, 1–12.
22. Sen, Z.; Eljadid, A.G. Rainfall distribution functions for Libya and Rainfall Prediction. *Hydrol. Sci. J.* **1999**, *44*, 665–680. [CrossRef]
23. Arora, K.; Singh, V.P. A comparative evaluation of the estimators of the log Pearson type 3 distribution. *J. Hydrol.* **1989**, *105*, 19–37. [CrossRef]
24. Moccia, B.; Mineo, C.; Ridolfi, E.; Russo, F.; Napolitano, F. Probability distributions of daily rainfall extremes in Lazio and Sicily, Italy, and design rainfall inferences. *J. Hydrol. Reg. Stud.* **2021**, *33*, 100771. [CrossRef]

25. Thevaraja, M.; Arampamoorthy, L. The Statistical Distribution of Annual Maximum Rainfall in Colombo District. *Sri Lankan J. Appl. Stat.* **2014**, *15*, 1765–1784.
26. Wilks, D.S. Comparison of three-parameter probability distributions for representing annual extreme and partial duration precipitation series. *Water Resour. Res.* **1993**, *29*, 3543–3549. [CrossRef]
27. Ahmad, I.; Abbas, A.; Saghir, A.; Fawad, M. Finding Probability Distributions for Annual Daily Maximum Rainfall in Pakistan Using Linear Moments and Variants. *Pol. J. Environ. Stud.* **2016**, *25*, 925–937. [CrossRef] [PubMed]
28. Hussain, Z. Rainfall Frequency Analysis Using Frechet and Log-Logistic Distributions of Sites of Azad Jammu and Kashmir, Pakistan. *Appl. Ecol. Environ. Res.* **2019**, *17*, 13607–13623. [CrossRef]
29. Hussain, F.; Nabi, G.; Wu, R.S. Spatiotemporal Rainfall Distribution of Soan River Basin, Pothwar Region, Pakistan. *Adv. Meteorol.* **2021**, *2021*, 6656732. [CrossRef]
30. Chaudhry, Q.Z. *Climate Change Profile of Pakistan*; Asian Development Bank: Manila, Philippines, 2017.
31. Sathar, Z.A.; Khan, K. *Climate, Population, and Vulnerability in Pakistan: Exploring Evidence of Linkages for Adaptation*; Population Council: Islamabad, Pakistan, 2019.
32. Ashraf, M.; Routray, J.K. Spatio-temporal characteristics of precipitation and drought in Balochistan province, Pakistan. *Nat. Hazards* **2015**, *77*, 229–254. [CrossRef]
33. New, M.; Hewitson, B.; Stephenson, D.B.; Tsiga, A.; Kruger, A.; Manhique, A.; Gomez, B.; Coelho, C.A.S.; Masisi, D.N.; Kululanga, E.; et al. Evidence of trends in daily climate extremes over southern and west Africa. *J. Geophys. Res. Atmos.* **2006**, *111*, 1–11. [CrossRef]
34. Redelsperger, J.; Thorncroft, C.D.; Diedhiou, A.; Lebel, T.; Parker, D.J.; Polcher, J. African monsoon multidisciplinary analysis (AMMA): An international research project and field campaign. *Bull. Am. Meteorol. Soc.* **2006**, *87*, 1739–1746. [CrossRef]
35. Ardoin, B.S. Hydroclimatic Variability and Impacts on Water Resources in Large River Basins in the Sudano-Sahelian Zone. Ph.D. Thesis, Sciences Et Techniques Du Languedoc T, Université Montpellier II, Montpellier, France, 2004.
36. Lienou, G. Impacts of Climate Variability on Water Resources and Transport of Suspended Matter in Some Representative Watersheds in Cameroon. Ph.D. Thesis, Universite De Yaounde I, Yaounde, Cameroon, 2007.
37. Aldughairi, A.A. Climate change assessment in middle and northern Saudi Arabia: Alarming trends. *DYSONA-Appl. Sci.* **2025**, *6*, 60–69. [CrossRef]
38. Lamptey, B. An analytical framework for estimating the urban effect on climate. *Int. J. Climatol.* **2009**, *30*, 72–88. [CrossRef]
39. Kouadio, K.; Bastin, S.; Konare, A.; Ajayi, V.O. Does convection-permitting simulate better rainfall distribution and extreme over Guinean coast and surroundings? *Clim. Dyn.* **2018**, *55*, 153–174. [CrossRef]
40. Pomeon, T.; Jackisch, D.; Diekkruger, B. Evaluating the performance of remotely sensed and reanalysed precipitation data over West Africa using HBV light. *J. Hydrol.* **2017**, *547*, 222–235. [CrossRef]
41. Nile, B.; Bayissa, Y. Evaluation of Satellite-Based Rainfall Estimates and Application to Monitor Meteorological Drought for the Upper Blue Nile Basin, Ethiopia. *Remote Sens.* **2017**, *9*, 669. [CrossRef]
42. Bichet, A.; Diedhiou, A. West African Sahel has become wetter during the last 30 years, but dry spells are shorter and more frequent. *Clim. Res.* **2018**, *75*, 155–162. [CrossRef]
43. Bichet, A.; Diedhiou, A. Less frequent and more intense rainfall along the coast of the Gulf of Guinea in West and Central Africa (1981–2014). *Clim. Res.* **2018**, *76*, 191–201. [CrossRef]
44. Carlos, L.B.; Rubén, D.M.; Francisco, J.C.L.; José, A.D.G. Validation of the accuracy of the CHIRPS precipitation dataset at representing climate variability in a tropical mountainous region of South America. *Phys. Chem. Earth Parts A/B/C* **2022**, *127*, 103184, ISSN 1474-7065. [CrossRef]
45. Wenqi, W.; Yungang, L.; Xian, L.; Yueyuan, Z.; Xuan, J.; Xue, L. Performance evaluation of the CHIRPS precipitation dataset and its utility in drought monitoring over Yunnan Province, China. *Geomat. Nat. Hazards Risk* **2019**, *10*, 2145–2162. [CrossRef]
46. Pelosi, A.; Chirico, G.B.; Furcolo, P.; Villani, P. Regional Assessment of Sub-Hourly Annual Rainfall Maxima. *Water* **2022**, *14*, 1179. [CrossRef]
47. Idate, S.S.; Mahale, D.M.; Bhange, H.N.; Gharde, K.D. Frequency Analysis for One day to Six Consecutive Days of Annual Maximum Rainfall for Mulde, Dist: Sindhudurg. *Int. J. Curr. Microbiol. App. Sci.* **2019**, *8*, 3069–3075. [CrossRef]
48. Bhatti, A.S.; Wang, G.; Ullah, W.; Ullah, S.; Hagan, D.F.T.; Nooni, I.K.; Lou, D.; Ullah, I. Trend in extreme precipitation indices based on long term in situ precipitation records over Pakistan. *Water.* **2020**, *12*, 797. [CrossRef]
49. Markovic, R.D. *Probability Functions of Best Fit to Distributions of Annual Precipitation and Runoff*; Colorado State University Hydrology Paper No. 8; Colorado State University: Fort Collins, CO, USA, 1965.
50. Salinas, J.L.; Castellarin, A.; Kohnova, S.; Kjeldsen, T.R. Regional parent flood frequency distributions in Europe-Part 2: Climate and scale controls. *Hydrol. Earth Syst. Sci.* **2014**, *18*, 4391–4401. [CrossRef]
51. Stendinger, J.R.; Vogel, R.M.; Foufoula, G.E. Frequency Analysis of Extreme Events. In *Handbook of Hydrology*, 1st ed.; Maidment, D.A., Ed.; McGraw-Hill: New York, NY, USA, 1993; Chapter 18, ISBN 0070397325.

52. Husak, G.; Michaelsen, J.; Funk, C. Use of the gamma distribution to represent monthly rainfall in Africa for drought monitoring applications. *Int. J. Climatol.* **2007**, *27*, 935–944. [CrossRef]
53. Dufour, J.M.; Farhat, A.; Gardiol, L.; Khalaf, L. Simulation-based Finite Sample Normality Tests in Linear Regressions. *Econ. J.* **1998**, *1*, 154–173. [CrossRef]
54. Arshad, M.; Rasool, M.T.; Ahmad, M.I. Anderson Darling and Modified Anderson Darling Tests for Generalized Pareto Distribution. *Pak. J. Appl. Sci.* **2003**, *3*, 85–88.
55. Seier, E. Comparison of Tests for Univariate Normality. *InterStat Stat. J.* **2002**, *1*, 1–17.
56. Conover, W.J. *Practical Nonparametric Statistics*, 3rd ed.; John Wiley & Sons, Inc.: New York, NY, USA, 1999; pp. 428–433.
57. Anderson, T.W.; Darling, D.A. A Test of Goodness-of-fit. *J. Am. Stat. Assoc.* **1954**, *49*, 765–769. [CrossRef]
58. Farrel, P.J.; Stewart, K.R. Comprehensive study of tests for normality and symmetry: Extending the Spiegelhalter test. *J. Stat. Comput. Simul.* **2006**, *76*, 803–816. [CrossRef]
59. Vogel, R.M.; Kroll, C.N. Low-Flow Frequency Analysis Using Probability-Plot Correlation Coefficients. *J. Water Resour. Plan. Manag.* **1989**, *115*, 338–357. [CrossRef]
60. Graedel, T.E.; Kleiner, B. Exploratory analysis of atmospheric data. In *Probability, Statistics and Decision Making in the Atmospheric Sciences*, 1st ed.; Murphy, A.H., Katz, R.W., Eds.; Westview: Boulder, CO, USA, 1985; pp. 1–43.
61. Nassif, W.G.; Al-Taai, O.T.; Mohammed, A.; Al-Shamarti, H.K.A. Estimate probability distribution of monthly maximum daily rainfall of Iraq. *J. Phys. Conf. Ser.* **2021**, *1804*, 012078. [CrossRef]
62. Panigrahi, B.; Paramjita, D.; Giri, M.; Paul, J. Frequency analysis for prediction of maximum flood discharge in Mahanadi River Basin. *Int. J. Curr. Microbiol. Appl. Sci.* **2020**, *9*, 3626–3639. [CrossRef]
63. Ng, J.L.; Yap, S.Y.; Huang, Y.F.; Noh, N.I.F.M.; Al-Mansob, R.A.; Razman, R. Investigation of the best fit probability distribution for annual maximum rainfall in Kelantan River Basin. *IOP Conf. Ser. Earth Environ. Sci.* **2020**, *476*, 012118. [CrossRef]
64. Shreyas, R.; Punith, D.; Bhagirathi, L.; Krishna, A.M.; Devagiri, G.M. Exploring different probability distributions for rainfall data of Kodagu—An assisting approach for food Security. *Int. J. Curr. Microbiol. Appl. Sci.* **2020**, *9*, 2972–2980. [CrossRef]
65. Younis, A.M. Regional flood frequency analysis for flood index estimation in hydrologic regions with limited flood data. *IOP Conf. Ser. Mater. Sci. Eng.* **2020**, *737*, 012161. [CrossRef]
66. Arvind, G.; Ashok Kumar, P.; Girish Karthi, S.; Suribabu, C.R. Statistical Analysis of 30 Years Rainfall Data: A Case Study. *IOP Conf. Ser. Earth Environ. Sci.* **2017**, *80*, 012067. [CrossRef]
67. Baghel, H.; Mittal, H.; Singh, P.K.; Yadav, K.; Jain, S. Frequency analysis of rainfall data using probability distribution models. *Int. J. Curr. Microbiol. Appl. Sci.* **2019**, *8*, 1390–1396. [CrossRef]
68. Bhavyashree, S.; Bhattacharyya, B.B. Fitting probability distributions for rainfall analysis of Karnataka, India. *Int. J. Curr. Microbiol. Appl. Sci.* **2018**, *7*, 1498–1506. [CrossRef]
69. Kumar, V.; Shanu; Jahangeer. Statistical distribution of rainfall in Uttarakhand, India. *Appl. Water Sci.* **2017**, *7*, 4765–4776. [CrossRef]
70. Vivekanandan, N. A comparative study of rainfall estimates using six statistical distributions. *AIP Conf. Proc.* **2007**, *923*, 88–99. [CrossRef]
71. Gul, S.; Ren, J.; Xiong, N.N.; Khan, M.A. Design and analysis of statistical probability distribution and non-parametric trend analysis for reference evapotranspiration. *PeerJ* **2021**, *9*, e11597. [CrossRef] [PubMed]
72. Sharafati, A.; Khazaei, M.R.; Nashwan, M.S.; Al-Ansari, N.; Yaseen, Z.M.; Shahid, S. Assessing the Uncertainty Associated with Flood Features due to Variability of Rainfall and Hydrological Parameters. *Adv. Civ. Eng.* **2020**, *2020*, 7948902. [CrossRef]
73. Ologhadien, I. Flood flow probability distribution model selection on Niger/Benue River Basins in Nigeria. *J. Eng. Res. Rep.* **2021**, *20*, 76–94. [CrossRef]
74. Niaz, R.; Almazah, M.M.A.; Zhang, X.; Hussain, I.; Faisal, M. Prediction for various drought classes using spatiotemporal categorical sequences. *Complexity* **2021**, *2021*, 7145168. [CrossRef]
75. Abro, M.I.; Zhu, D.; Khaskheli, M.A.; Elahi, E.; Ramay, M.A.U.H. Statistical and qualitative evaluation of multi-sources for hydrological suitability inflood-prone areas of Pakistan. *J. Hydrol.* **2020**, *588*, 125117. [CrossRef]
76. Hanwat, S.; Pal, K.; Panda, K.C.; Sharma, G.; Mandloi, S.; Tripathi, V.K. Flood frequency analysis for Burhi Gandak River Basin. *Int. J. Enviornment Clim. Change* **2020**, *10*, 82–89. [CrossRef]
77. El-Aal, A.A.; Radwan, A.E.; Abdelshafy, M.; Omaar, A.E.; Youssef, Y.M. A Synergistic Use of Remote Sensing and Hydrodynamic Techniques for Flash Flood Mitigation Toward Sustainable Urban Expansion in Najran Valley, Saudi Arabia. *Earth Syst. Environ.* **2024**, *8*, 465–482. [CrossRef]
78. Reggiani, P.; Boyko, O.; Rientjes, T.; Khan, A. Probabilistic precipitation analysis in the central Indus River Basin. In *Elsevier eBooks*; Elsevier: Amsterdam, The Netherlands, 2019; pp. 101–121. [CrossRef]
79. Zaman, M.; Ahmad, I.; Usman, M.; Saifullah, M.; Anjum, M.N.; Khan, M.I.; Qamar, M.U. Event-Based Time Distribution Patterns, Return Levels, and Their Trends of Extreme Precipitation across Indus Basin. *Water* **2020**, *12*, 3373. [CrossRef]

80. Mumtaz, M.; Jahanzaib, S.H.; Hussain, W.; Khan, S.; Youssef, Y.M.; Qaysi, S.; Abdelnabi, A.; Alarifi, N.; Abd-Elmaboud, M.E. Synergy of Remote Sensing and Geospatial Technologies to Advance Sustainable Development Goals for Future Coastal Urbanization and Environmental Challenges in a Riverine Megacity. *ISPRS Int. J. Geo-Inf.* **2025**, *14*, 30. [CrossRef]
81. Naz, F.; Dars, G.H.; Ansari, K.; Jamro, S.; Krakauer, N.Y. Drought trends in Balochistan. *Water* **2020**, *12*, 470. [CrossRef]
82. Ahmed, A.; Mohammad, N.; Wadood, A. Balochistan: Overview of its Geo-economic and Socio-economic Perspectives. *Rev. Appl. Manag. Soc. Sci.* **2020**, *3*, 235–246. [CrossRef]
83. Ahmed, K.; Shahid, S.; Ali, R.; Harun, S.; Wang, X.J. Evaluation of the performance of gridded precipitation products over Balochistan Province, Pakistan. *Desalination Water Treat.* **2017**, *79*, 73–86. [CrossRef]
84. Alam, F.; Salam, M.; Khalil, N.A.; Khan, O.; Khan, M. Rainfall trend analysis and weather forecast accuracy in selected parts of Khyber Pakhtunkhwa, Pakistan. *SN Appl. Sci.* **2021**, *3*, 575. [CrossRef]
85. Jehan, I.; Atta-Ur-Rahman; Waqas, T. Assessment of meteorological drought and trend detection in Khyber Pakhtunkhwa, Pakistan. *Arab. J. Geosci.* **2020**, *13*, 765. [CrossRef]
86. Javed, Z.H.; Khan, S.; Wahid, A.; Ranjha, A.N.; Hassan, M.U. Climate of the Gilgit-Baltistan Province, Pakistan. *Int. J. Econ. Environ. Geol.* **2020**, *11*, 16–21. [CrossRef]
87. Baig, S.U.; Rehman, M.U.; Janjua, N.N. District-level disaster risk and vulnerability in the Northern mountains of Pakistan. *Geomat. Nat. Hazards Risk* **2021**, *12*, 2002–2022. [CrossRef]
88. Nabeel, A.; Athar, H. Observed, stochastically simulated, and projected precipitation variability in Pakistan. *Theor. Appl. Climatol.* **2018**, *137*, 2239–2256. [CrossRef]

Disclaimer/Publisher's Note: The statements, opinions and data contained in all publications are solely those of the individual author(s) and contributor(s) and not of MDPI and/or the editor(s). MDPI and/or the editor(s) disclaim responsibility for any injury to people or property resulting from any ideas, methods, instructions or products referred to in the content.